Prediction of Fatigue Crack Growth Rate using Optimized Neural Networks

HASSAAN BIN YOUNIS

NUST201464531MCEME35514F

Supervisor

DR. AMIR HAMZA

DEPARTMENT OF MECHATRONICS ENGINEERING

COLLEGE OF ELECTRICAL & MECHANICAL ENGINEERING

NATIONAL UNIVERSITY OF SCIENCES AND TECHNOLOGY

ISLAMABAD

MARCH, 2018

Prediction of Fatigue Crack Growth Rate using Optimized Neural Networks

Author

HASSAAN BIN YOUNIS

NUST201464531MCEME35514F

A thesis submitted in partial fulfillment of the requirements for the degree of

MS Mechatronics Engineering

Thesis Supervisor:

DR. AMIR HAMZA

Thesis Supervisor's Signature:

_____

DEPARTMENT OF MECHATRONICS ENGINEERING

COLLEGE OF ELECTRICAL & MECHANICAL ENGINEERING

NATIONAL UNIVERSITY OF SCIENCES AND TECHNOLOGY, ISLAMABAD

MARCH, 2018

Declaration

I officially state that the research work with a title "*Prediction of Fatigue Crack Growth Rate using Optimized Neural Networks"* is my individual work. This research work has not been introduced anywhere else for evaluation. The research work used from past sources of other authors is appropriately recognized and referenced

Student's Signature

HASSAAN BIN YOUNIS

NUST201464531MCEME35514F

Language Correctness Certificate

It is officially stated that this thesis has been examined by an English language expert and does not contain any typing, syntax, semantic, grammatical and spelling errors. This thesis is also compiled in accordance with the format advised by the institute.

Student's Signature

HASSAAN BIN YOUNIS

NUST201464531MCEME35514F

Supervisor's Signature

DR. AMIR HAMZA

Copyright Statement

Acknowledgements

I am grateful to The Creator of this universe Allah Almighty to have guided me for the duration my life and in this work at each progression and for every new idea which He setup in my mind to enhance it. In reality, I could have finished nothing without His invaluable help and direction. Whoever helped me over the span of my thesis, regardless of my parents or any other person was His will, so for sure none be deserving of acclaim however You.

I am bountifully grateful to my dearly loved parents and relatives who brought me up when I was not equipped of walking on feet and kept on supporting me ethically and monetarily all through in each department of my life. Whatever I am today is because of their prayers.

I might likewise want to express extraordinary gratitude to my supervisor Dr. Amir Hamza for his guidance all through my thesis. I am particularly appreciative to Dr. Khurram Kamal for indicating individual attention, wonderful support and collaboration in this thesis. He by and by observed me throughout experimentation stage. Each time I got stalled out in something, he thought of an arrangement. Without his guidance I wouldn't have possessed the capacity to conclude my thesis. I value the understanding and direction of my supervisor and co-supervisor all through the entire thesis. I can undoubtedly claim that they are more than instructor and adviser for me.

I would likewise want to say thanks to Brig. Dr. Javaid Iqbal and Dr. Umar Shahbaz for being on my thesis direction and evaluation board. I would likewise want to say thanks and recognize the hard work of Muhammad Fahad Sheikh and Tayyab Zafar for their assistance amid thesis. I might want to state my unique appreciation to my beloved course fellows Muhammad Rizwan Qayyum and Muhammad Usman for their help.

In conclusion, I likewise want to offer my thanks to every one of the people who have rendered significant support during my research work.

ABSTRACT

In aerospace industry, Fatigue Crack Propagation pose a serious threat to the professionals involved in designing mechanical assembly of the aircraft structures. In these structures crack growth is a problem to be handled seriously as human life risk is concerned in addition to economic loss. Fatigue Crack Growth (FCG) Rate is the rate at which crack grows with number of cycles subjected to constant amplitude loading. FCG curve is drawn between crack growth rate on y-axis and SIF range on x-axis. It must be predicted accurately to avoid losses. Upon analyzing the curve it becomes obvious that the correlation between Stress Intensity Factor (SIF) range "ΔK" and FCG rate "da/dN" is non-linear even in Paris Region (Region II). Empirical formulation methods are unable to handle non-linearity satisfactorily. Other hybrid techniques are also found incapable of dealing with non-linearity suitably. In contrast to the prior methods, machine learning algorithms are capable to deal with the non-linearity issue in a much better way owing to their admirable learning ability and flexible nature. In this research work three distinct MLA based Optimized Neural Networks are utilized for prediction of FCG rate. The used algorithms include Genetic Algorithm based Optimized Neural Network, Hill Climbing based Optimized Neural Network and Simulated Annealing based Optimized Neural Network. The algorithms presented in the proposed technique are validated by testing on different aluminum alloys used for aerospace industry that includes 2324-T39, 7055-T7511 and 6013-T651 aluminum alloys. The minimum predicted MSE for 2324-T39 aluminum alloy is achieved by Simulated Annealing based Optimized Neural Network that is $\mathbf{1.0559 \times 10^{-9}}$. For 7055-T7511 alloy, minimum predicted MSE is $\mathbf{1.4284 \times 10^{-9}}$ which is achieved by Hill Climbing based Optimized Neural Network. Finally, the least predicted MSE for 6013-T651 is $\mathbf{3.1069 \times 10^{-8}}$ achieved by Hill Climbing based Optimized Neural Network. Taking all alloys on which experiments were held with used algorithms, the minimum predicted MSE is achieved as $\mathbf{1.0559 \times 10^{-9}}$ for 2324-T39 Aluminum Alloy with Simulated Annealing based Optimized Neural Network. Moreover, the results show an exceptional conformity to experimental data.

Keywords: *Fatigue Crack Growth Rate, Optimized Neural Network, Genetic Algorithm, Hill Climbing, Simulated Annealing*

Table of Contents

List of Figures

List of Tables

1. INTRODUCTION

This chapter presents an introduction to fatigue crack growth rate and the science involved in prediction of fatigue crack growth rate using different techniques while taking into account the importance of accurate prediction keeping in mind the life risk involved in case of any accident due to material failure, problem statement, aim of the research and the motivation behind the topic.

1.1. Introduction to Thesis

The major cause of most of the failure of engineering components is material failure which may lead towards fatal consequences. These material failures are the results of excessive fatigue induced inside the structures. Initiation and propagation of crack in an engineering component as a result of fatigue leads towards catastrophic results which may include causalities as well. Fatigue failure has been the subject of consideration of experts for more than 150 years. As fatigue failure has got better awareness during last 50 years, it has come out while investigating accidents that it was the major cause in most of the tragic accidents. The breakage of an axle due to excessive stresses in leading locomotive, causing the derail of engine in Versailles Train Crash in 1842, decompression with an explosion over Mediterranean Sea of two flights and fatalities of all the passengers in De Havilland Comet Plane Crashes in 1954 and derail of a high speed train due to wheel failure in Eschede Train Disaster in 1998 are some of the examples in which material failure resulted into disastrous consequences.

While analyzing fatigue failures, it can be observed that these types of failures can be divided into three different categories [1]; Stress based, strain based and fracture mechanics based. Stress based approach is focused on the average stresses on the areas prone to fatigue while studying fatigue life. Strain based approach is focused on treatment of confined plastic yielding that occur mostly around edges and notches. Fracture mechanics approach is what this research work is based upon. It is discussed in detail as followed

Fracture mechanics is the branch of mechanics that cater for the displacement discontinuities in materials as a result of fatigue with the distinctive consideration to their progression. Usually, the application of load that guides to the engagement of crack propagation is applied in any type from the three modes. i.e. opening, sliding or tearing manner. It is shown in the Figure 1.1.

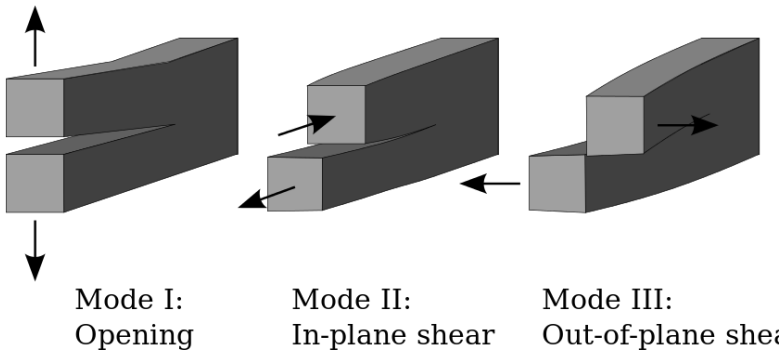

Figure 1.1. Modes of failure during engagement of crack propagation

Fracture mechanics approach can be further divided into two different categories. The first one is called a lifetime approach in which total number of cycles are calculated that lead to failure. The other one is called damage tolerance approach which is defined as the fatigue crack growth (FCG) caused as a result of repeated cyclic loading [1].

For about last 60 years, experts have been studying early detection of cracks and estimating fatigue life of materials. Fatigue life is divided into two phases. There is crack initiation phase which is termed as the largest duration phase of fatigue life which is caused by high cycle fatigue followed by crack growth which is caused by low cycle fatigue is the most significant phase of fatigue life [2]. Different fatigue life phases are shown in figure 1.2.

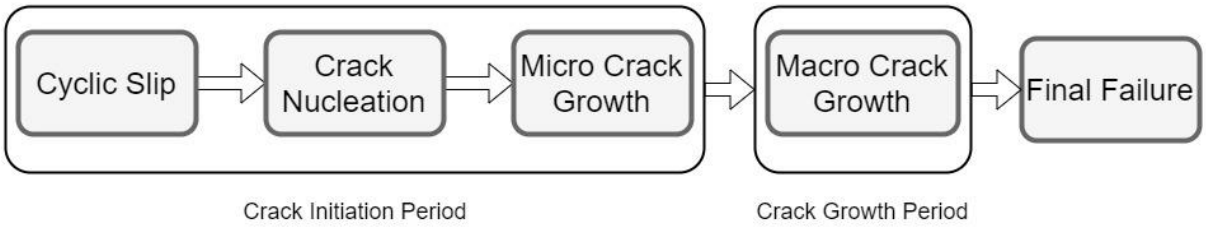

Figure 1.2. Different phases of fatigue life

The accidents due to material failure in the past urged the experts in this sector to predict fatigue crack growth rate in order to estimate the life of an engineering component. Due to life risk involved it is very critical to estimate the life of material accurately. For it fatigue crack growth rate needs to be predicted accurately. Many researchers came up with their models that included empirical formulas [3-5].The behavior of FCG is explained by crack growth rate da/dN and stress intensity factor range ΔK. The characteristic curve is plotted with ΔK lying with respect to x-axis while da/dN resting with respect to y-axis. In the above mentioned equations, a is termed as crack length while N is termed as the number of cycles. FCG graph is separated into 3 regions. Region II is most important to be focused where the relationship between the variables on x-axis and y-axis is considered to be linear but after various experiments on different materials, it can be inferred that the relationship is non-linear even in Paris region (region II). This behavior is more obvious in some materials and less in others. Analytical techniques have proved to be unable to address this non-linear relationship satisfactorily. To address this non-linearity, many exponential models that were derived from the theory of Linear Elastic Fracture Mechanics (LEFM) are also proposed. Upon unsatisfactory response of classical models, hybrid models were presented by researchers. Numerical approach combined with machine learning algorithms are most prominent in this case. Machine learning methods have proved to be an alternative and most interesting approach because of their capability while catering the case because of their excellent flexibility and approximation to non-linear and multi-variable problems. These algorithms include Back Propagation Algorithms, Relevance Vector Machine (RVM), Recurrent Neural Networks (RNN), Particle Swarm Optimization (PSO), Optimized Artificial Neural Networks etc. due to the generalization and learning ability, the professionals have been using these networks in different fatigue problems as well.

In this research work, regression based models of machine learning methods have been used for accurate prediction of fatigue crack growth rate. These algorithms are applied on different aluminum alloys especially used in aircraft structures. The results obtained are compared with experimental data to check accuracy of algorithms. The predicted results have been observed to be much closer to experimental data

The thesis is organized in following sections. Chapter 2 presents the previous work related to fatigue crack growth rate including empirical models, hybrid models and prediction using machine learning algorithms. Chapter 3 explains the background theory while chapter 4 and chapter 5 explain the experimental setup and data acquisition, and the results and detailed discussion respectively. Chapter 6 discusses the challenges related to implementation of the proposed technique and future work.

1.2. Summary

- The major cause of most of the failure of engineering components is material failure which may lead towards fatal consequences. As fatigue failure has got better awareness during last 50 years, it has come out while investigating accidents that it was the major cause in most of the tragic accidents.
- While analyzing fatigue failures, it can be observed that these types of failures can be divided into Stress based, strain based and fracture mechanics based failures. Fracture mechanics approach is what this research work is based upon. Fracture mechanics is the field of mechanics that deals with the displacement discontinuities in materials as a result of fatigue with the distinctive consideration to their progression.

- In order to predict fatigue crack growth rate accurately many empirical and analytical models including hybrid approach have been proposed but they have not addressed the problem satisfactorily. Machine learning methods have proved to be an alternative and most interesting approach because of their capability while catering the case because of their excellent flexibility and approximation to non-linear and multi-variable problems.

2. LITERARTURE REVIEW

This chapter contains a discussion of various models that have been used for the prediction of fatigue crack growth rate in the materials specifically used in aircraft industry. Previously used techniques which involve empirical and analytical relations, machine learning based methods and hybrid models are discussed keeping in view the non-linearity factor in FCG curve.

2.1. Introduction to Fracture Mechanics and Fatigue Crack Growth Models

Fatigue crack growth models based on theory of fracture mechanics are generally developed using experimental data using curve fitting parameters of the form [2].

$$\frac{da}{dN} = f(\Delta K, R) \qquad 2.1$$

Where ΔK is the stress intensity factor range and R is the stress ratio

$$K = F\partial\sqrt{\pi a} \qquad 2.2$$

Where F is termed as geometric factor and is a variable that depends upon the relative crack length $\alpha = {}^{a}/_{b}$. a is the crack length

Different researchers proposed different models to predict fatigue crack growth rate in the materials. Some used analytical methods whereas other used machine learning based methods or hybrid models to predict crack propagation. Following are the techniques proposed by various researchers.

Paris et al. [3] questioned the claim about validation of a crack-propagation theory. He claimed that these laws were inferred carrying experimentation on limited amount of data based on few specimens by saying that it is a destitute assessment of any model. He along with his fellow researchers gathered a wider spread range of test data and used it for in depth analysis of crack propagation laws. Initially, they look over and assessed crack-propagation laws quoted at that time. After that, the imprecise results achieved by the comparison of laws based on a narrower assortment of test data were compared with a

wider range of convenient data. The results disclosed that using limited range of data is not a gentle assessment of a crack-propagation laws legitimacy. For this, the authors suggested that laws which relate an ample range of data, from many specimens are operably the "perfect" laws.

Forman et al. [4] proposed an improved method in order to analyze crack growth rate subjected to cyclic loading. His claim was stress intensity factor range ΔK is the controlling factor of crack propagation rate. This theory addressed different important factors like load ratio Randunsteadiness of SIF upon realization at critical value which is also known as fracture toughnessK_c. These parameters were ignored in the previous models proposed by other researchers. By using this theory combined with numerical integration approach with the assistance of computing device, a claim was made that more accurate results for prediction of FCG rate had become possible to obtain for the structures prone to cyclic loading. Forman model can be mathematically represented as given by the following equation

$$\frac{da}{dN} = \frac{C_F(\Delta K)^{my}}{(1-R)\left(K_c - K_{\_\max}\right)} \qquad 2.3$$

Where K_c is the fracture toughness. It is used to explain crack growth at higher rates.
Keeping in view the drawbacks in the previous models, Priddle [5] presented his model by taking into consideration, the important parameters like ΔK_{th} and K_c. In his research work crack propagation process was defined beneath various stress intensity conditions. The results were conceded out using a specimen of mild steel under ambient temperature. The claim was made that this model can fit the non-linearities in all the three regions of FCG curve but in any case, the most important disadvantage in this method is that it doesn't accommodate for R-ratio effects.

Walker [6] proposed a model as an improvement to Paris [3] model. Paris ignored the effect of stress ratio, R due to which his model could not address non-linearity in FCG curve. Walker proposed a factor called stress intensity factor range, ΔK. He explained that this parameter is considered to be an equivalent zero ($R = 0$)up to maximum SIF and it has the

same result on Fatigue Crack Growth rate as K_{max} and R combined showed. After this improvement his model can be represented as given by following relationship

$$\frac{da}{dN} = C_W(\overline{\Delta K})^{m_W} \quad 2.4$$

$$\frac{da}{dN} = C_W\left(\frac{\Delta K}{(1-R)^{1-\gamma W}}\right)^{m_W} \quad 2.5$$

$$\Delta K = K_{max}(1-R) \quad 2.6$$

Where C_W and m_W are the constants similar to the constants C_P and m_P that are used in Paris model. $\overline{\Delta K}$ is the parameter that causes same crack growth rate as the two parameters K_{max} and R have the combined effect. γW is specific for material.

Elber et al. [7], on the basis of the contrivance upon which fatigue crack grows presented the concept of crack closure effect. He explained that under the time period of cyclic loading in tension, crack induced as a result of fatigue lead to cessation by its own provided that the load applied is half the maximum load. Experiments were carried out using 2024-T3 aluminum alloy sheet and crack propagation was observed under constant amplitude loading. Furthermore, it was projected that acceleration and retardation effects throughout the process of crack growth can also be studied under capricious amplitude loading by means of this crack closure concept. This model had abenefit that it could not only be applied to three regions of crack propagation but it includes stress ratio effects and other parameters ignored earlier. The major weakness in this prototypical is that hypothetically this model only covers narrower range of stress ratio, R.

Kujawski [8] introduced a new concept of mechanical driving force to study long and short crack propagation rate. Instead of using moot crack closure concept data, a new parameter ($\sqrt{(\Delta K^{+}K_{max})}$) is proposed in this research work where ΔK^{+} is geometric mean of positive values of SIF range and K_{max} is the maximum value of SIF data. The results were verified using six aluminum alloys. Donald et al. [9] and Sadananda et al. [10] used

mechanical driving force concept to propose their techniques as an improvement of previous models

Based on the previous research,Kujawski et al. [11] suggested a method to predict stress-ratio effects on fatigue crack growth rate. This method is named as K* method where K* is the fatigue crack driving force. Mathematically, K* and fatigue crack growth rate can be expressed as:

$$K^* = (K_{max})^{\alpha}(\Delta K^+)^{1-\alpha} \quad 2.7$$

$$\frac{da}{dN} = f\,(K^*) \quad 2.8$$

Where α is correlation factor, and ΔK^+ is the positive portion of appliedΔK. In correspondence with the aforementioned learning, this methodology is correspondingly operative or improved as takes into account K_{max} and K^+ as it remarkably pacts with the non-linearity in region II. The major drawback of this method is that it cannot calculate the correlation factor, α and R-ratio effects for diverse materials perfectly in all the three regions of da/dN - ΔK curve.

As the problem is discovered, a number of researchers have been pugnacious to provide an analytical formula in order to solve the non-linearities during the prediction of FCG rate. In the efforts to do so, many parameters likeΔK_{eff},ΔK_{th},K_c and$R$ are convoluted. In reality, mathematical formularies are obstinate to answer natural and multi-variable complications, it is very hard to find out a special and general analytical relationship for these circumstances. The problem could not be addressed by analytical formulas. To overcome the limitations, other ways were explored by researchers as a result of which more multidisciplinary methods were brought together. Midst others, numerical approach and machine learning methods are ascertained to be most operative. A hybrid approach combining numerical methods and machine learning algorithms is also presented in different ways.

Sukumar et al. [12] presented a particular mathematical methodology for planar 3D FCG simulations. They proposed a method that combined the Extended Finite Element Method

(X-FEM) to the Fast Marching Method (FMM). In the X-FEM, an alternating function together with the 2-D asymptotic crack-tip dislocation welds along with the finite element approximation were considered in order to deal with the crack by the application of the concept of Partition of Unity. It made the domain possible to be displayed by finite components without unambiguous meshing of the crack surface. The FMM in combination with the Paris crack growth law was utilized to propel the crack front. SIF for planar 3-D cracks were processed, and FCG simulations taking planar cracks under consideration were proposed. Good understanding between the mathematical outcomes and theory was obtained. Mode I troubles of penny and elliptical cracks in an infinite field were tackled. The numerical SIFs were observed to be in good concurrence with the perfect answer to these problems.

Chopp et al. [13] proposed a numerical technique for modeling fatigue crack propagation of multiple coplanar cracks. They merged the extended finite element method (X-FEM) to the fast marching method (FMM). The entire crack geometry, including one or more cracks was represented by a single signed distance (level set) function. The FMM in conjunction with the Paris crack growth law was used to advance the crack front. Finally, simulations for multiple planar cracks were presented, with crack merging and fatigue growth carried out without any user-intervention or remeshing.

Bui et al. [14] established an effective and enhanced Knowledge Based Neural Network (KBNN) and combined with finite element analysis (FEA)based on empirical and ANN modeling in order to forecast spring back angles in metal sheet bending more precisely. During experimentation U and V type bends are processed. It showed better results when compared with previously presented models.

Bhattacharya et al. [15] used extended finite element method (XFEM) to examine crack growth in case of interfacial cracks in bi-layered materials. A specimen of bi-material is double layered having two distinct materials with a bottom layer consisting of aluminum alloy and graded material designed functionally is used in upper layer. The graded material layer designed functionally has 100% aluminum alloy and 100% ceramic on the right side.

The graded segregation in characteristics of the material of the FGM layer is expected to be exponential throughout the alloy flank up to the ceramic flank. The dominion based interaction integral methodology is prolonged. The aim is to achieve the SIF for a crack at interface subjected to thermo-mechanical loading. The fatigue life of the interfacial cracked specimen is attained by the use of the Paris law of FCG subjected to cyclic Mode-I, thermal and mixed-mode loads. The research disclosed the propagation of crack into the FGM layer when subjected to any of the types of loads.

Hu et al. [16] proposed a new technique of singular finite element analysis which includes fracture process zone (FPZ) lying in front of crack tip by utilizing cohesive zone model (CZM) subjected to variable amplitude cyclic loading. The aim was to learn fatigue crack growth under variable amplitude cyclic loading as previous attempts were focused on developing models to the problem in which Plastic Zone Length (PZL) cracks were involved. The claim of accurate forecast of fatigue life of materials underneath the application of variable amplitude cyclic loading is proved using the mentioned approach. Machine learning methods are ascertained to be most remarkable and accomplished when problem of linearity is taken into account due to their robustness and estimation to non-linear and multi-variable complications. Amongst those algorithms, Relevance Vector Machine (RVM), back propagation algorithms, Recurrent Neural Network (RNN), fuzzy logic, neural-fuzzy system and particle swarm optimization (PSO) are noticeable.

Mohanty et al. [17] proposed the prediction of fatigue crack propagation life of 7020-T7 and 2024-T3 aluminum alloys using Artificial Neural Networks (ANN) undergone due to load ratio effects. After various phenomenological techniques for estimation of fatigue life of materials, an automated prediction method was proposed in this research. A prodigious prospect is shown by ANNs for fatigue life prediction when interpolating between tested span and results show an outstanding agreement with experimental data but this model is incapable to deal satisfactorily when data is extrapolated

Rodríguez et al. [18] made the use of Artificial Neural Networks in order to estimate useful life of blades of steam turbine. The network was designed with six input neurons, three

hidden layer neurons and an output neuron where hidden and output layers are designed with sigmoidal and linear transfer function respectively. In this research it was shown that all the concerned factors which include mean stress, resonance stress, damping strength, frequency ratio and dynamic stress contribute towards prediction of useful life of blades. However, resonance stress has the largest effect with comparative significance of 35% trailed by frequency ratio and others.

Rafiq et al. [19] demonstrated the use of neural networks in various engineering applications. Everyday procedures to design the network to be used in different engineering applications are also discussed. After comprehensive introduction of neural networks, various aspects of mainly three types of neural networks is discussed. This types include multi-layer perceptron (MLP), radial basis network (RBF) and normalised RBF (NRBF).

Venkatesh et al. [20] used back-propagation network for perfect life prediction of materials exposed to creep-fatigue behavior at raised temperature. He demonstrated his idea using nickel based alloy($ICONEL690$). The network was designed with six input layer neurons, two hidden layer neurons and an output layer neuron with eleven training groups and finite reiterations(< 20000). The proposed model was compared with Cofin-Manson, Linear Life Fraction and Hysteresis Energy Prediction techniques and noteworthy enhancement was witnessed.

Artymiak et al. [21] proposed a model of calculation of fatigue strength and estimation of fatigue perimeter using classification based artificial neural networks. After the preparation of comprehensive database by applying tests on specimen, data is divided into six different classes after which classifier is applied. It was seen in this research that prediction by the use of ANNs showed better results than previous methods. The obtained results are much closer to the desired results.

Kang et al. [22] used back-propagation neural network for determination of the crack opening load from discrepantly displaced signal curves. A three layer network was engaged and arrangements of crack opening stages and S/N ratios were made through

computer simulations. The proposed methodology was applied to constant amplitude loading tests and showed good accuracy with desired results

Haque et al. [23] proposed a model based on artificial neural network for fatigue crack growth rate of dual phase steel as a result of corrosion. The DP steel specimen consisted of 32-76% martensite stuffing. The proposed model had an excellent contrast with experimental results.

Cheng et al. [24] presented a model of on-line corrosion of fatigue crack growth monitoring using artificial neural network. The advantage of this model is that it only needs crack length, a and number of loading cycles, N and it is not material or environment specific. The model is validated through various examples.

Zio et al. [25] utilized a Bayesian elaboration of Support Vector Machine (SVM) also called Relevance Vector Machine (RVM) in order to give a prediction of the remaining useful life of a structure under a safety-critical standard. In contrast to other methods it was claimed that this proposed model had better performance considering computational mandate, data requirements and precision.

Mohanty et al. [26] proposed a genetic algorithm in order to predict fatigue life of a material. He demonstrated it using 2024-T3 aluminum alloy. FCG rate was designed by the use of exponential methodology from experimental crack length, a and number of cycles, N data and afterwards utilized to develop training data base for proposed model devising accompanied with R-ratio, maximum SIF, K_{max} and SIF range, ΔK. This model was compared with other presented neural network models and was in close agreement with desired results.

Zhang et al. [27] used an ANN based algorithm, Radial Basis Function Neural Network (RBF-NN) to propose a fatigue life prediction model. The data to be tested is subjected to constant amplitude loading test with different stress ratios. The obtained results were

compared with Forman and Wheeler models and delivered better agreement with experimental data.

Wang et al. [28] compared three MLA based algorithm in order to forecast FCG rate. These include Extreme Learning Machine (ELM), Radial Basis Function Neural Network (RBF-NN) and Genetic Algorithm based Back Propagation Network (GABP-NN). The acquired outcomes were contrasted with one another in addition to comparing them with classical methodology. i.e. K* approach). The gained outcomes from MLA based methods were found to be improved in accuracy than classical methodology. The least Predicted MSE was obtained with ELM i.e. 1.33×10^{-8} for 2024-T351 Aluminum Alloy. ELM had come out to be most accurate among others.

2.2. Summary

The discussion in this chapter can be summarized as follows

- Fatigue crack growth models presented in the past are based on theory of fracture mechanics.
- Different researchers proposed different models to predict fatigue crack growth rate in the materials. Some used analytical methods whereas other used machine learning based methods or hybrid models to predict crack propagation
- Various analytical models have been presented that are based on the theory of Linear Elastic Fracture Mechanics. Amongst them Paris questioned the claim about validation of a crack-propagation theory by claiming that previous laws were presented based on the limited range of data and presented his model that was based on a wider range of data and were called “Perfect Laws”
- Prominent hybrid techniques used for FCG applications are also discussed. These techniques include numerical simulation combined with machine based algorithms. Extended Finite Element Analysis based model are also discussed in this chapter
- Different Machine Learning based classifiers used for prediction of Fatigue Crack Growth Rate have been reviewed from literature. Different classification and regression based models have been employed for FCG monitoring and prediction applications.

3. TOOLS AND TECHNIQUES

This chapter describes the techniques used to accomplish the ranges of thesis as well as the background theory linked to them. The chapter is distributed into different sections; introduction to fracture mechanics, artificial neural networks theory and machine learning techniques used in the study. The way these techniques are applied is also enlightened.

3.1. Introduction to Fracture Mechanics

All engineering apparatuses and structures are open to geometrical incoherence. These disruptions comprise of strung connections, spacing for windows that exist in airplane fuselages, keyways in shafts, teeth of gear wheels and many more. The dimension and form of these machineries are perilous as they decide about the power of the curio. Conventionally, the strength of portions or assemblies encompassing defectiveness is measured by evaluating the stress concentration produced by intermittent features. To sketch it, consider the associated four cases:

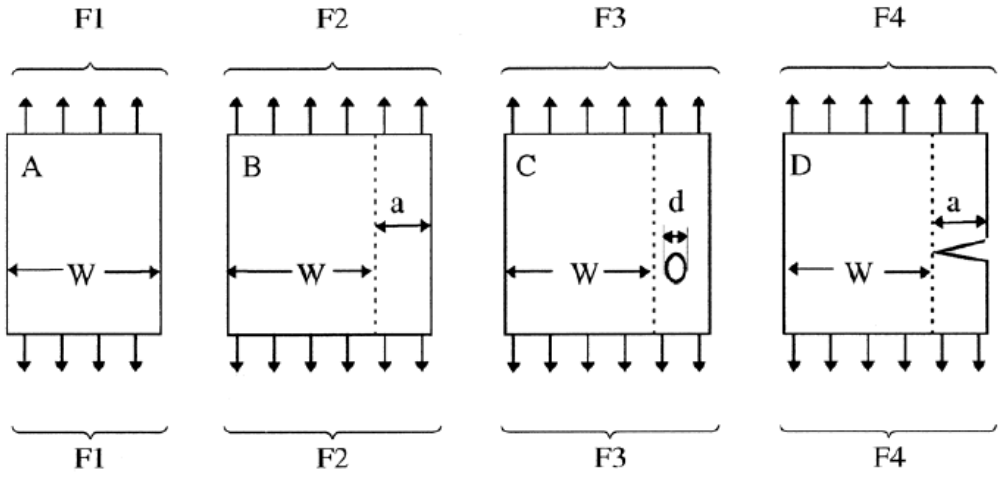

Figure 3.1. Comparison of forces on a plate under different conditions [2]

The thickness of each plate is the same. The force required to break the above mentioned four samples can be organized in the order as arranged below:

$$F4 < F3 < F1 < F2 \qquad 3.1$$

Fracture mechanics is explained as an arrangement of hypotheses depicting the conduct of solids or structures with geometrical irregularities at the size of the structure. The abnormality in features may be as line discontinuities in two-dimensional media, (for instance, plates and shells) and surface discontinuities in three-dimensional media. Presently, in materials science, fracture mechanics is an essential gadget used to upgrade the execution of mechanical parts. It incorporates the physics of stress and strain direct of materials, particularly the theories of elasticity and plasticity. The forecast of crack propagation is at the heart of the damage tolerance when mechanical design is under consideration. Normally, the force is applied by the following three methods to engage crack propagation.

3.2. Linear Elastic Fracture Mechanics

Fracture mechanics is mainly categorized as Linear Elastic Fracture Mechanics (LEFM) and

Elasto-Plastic Fracture Mechanics (EPFM). LEFM gives tremendous results for brittle-elastic

materials that include high-strength steel, glass, ice, concrete, etc. On the other hand, plasticity will always go before fracture for ductile materials.

3.2.1.Stress intensity factor

During the World War II, Irwin [29] turned out to be involved in the crack of steel shell coating for the period of infiltration during firing. Experimental work was completed at the U.S. Naval Research Laboratory in Washington, D.C. this research [30] led to a theoretic design of crack that carry on to discover widespread applications. Irwin showed that the stress field $\sigma(r, \theta)$ in the locale of an considerably sharp crack tip possibly can be termed as:

$$\sigma_{yy} = \frac{K_I}{\sqrt{2\pi r}} cos\frac{\theta}{2}(1 - sin\frac{\theta}{2}sin\frac{3\theta}{2}) \quad \textbf{3.2}$$

Where K_I can be expressed as:

$$K_I = \sigma_a Y\sqrt{\pi c} \quad \textbf{3.3}$$

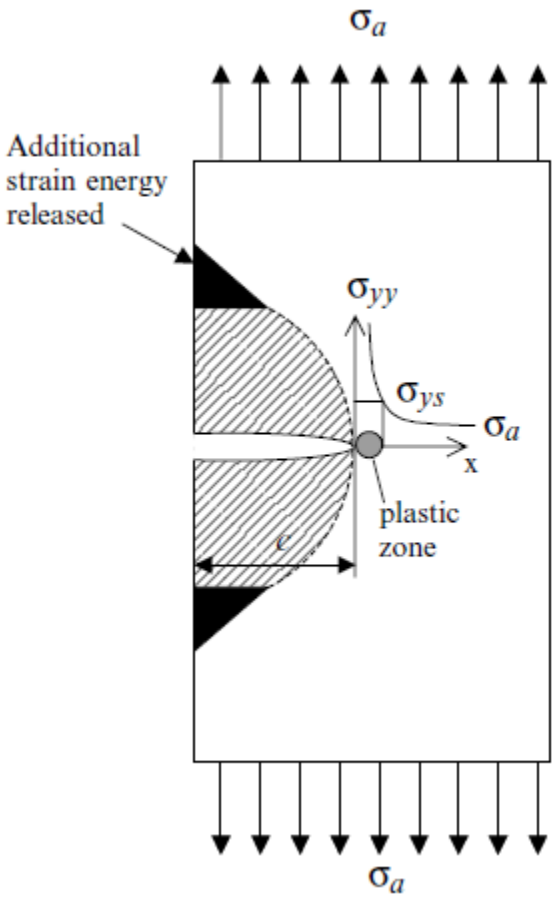

Figure 3.2. Semi-infinite plate subjected to a homogenously applied stress with single-ended exterior crack of length c/2.

3.2.2.Crack tip plastic zone

From equation 3.2, it is clear that at the crack tip (i.e. r = 0),σ_{yy} approaches infinity. Though, in actual, the stress at the crack tip is inadequate to the yield strength of the material, henceforth linear elasticity cannot be presumed inside a definite distance of the crack tip. This non-linear state is also termed as "Crack Tip Plastic Zone [31]". Outside this zone, dislodgments underneath the superficially functional stress typically observes Hooke's law, and the equations of linear elasticity are applicable. The elastic material outside the plastic region spreads stress to the material inside the region, whereas non-linear actions happen that might impede the stress area from being resolute accurately. Equation 3.2demonstrates that the stress is proportionate to $\sqrt{1/r}$. The straining energy release rate is not prejudiced by procedures inside the plastic district if the plastic region is comparatively lesser. It is clear that an estimated scope of the plastic region is given by:

$$r_P = \frac{K_I^2}{2\pi\sigma_{ys}^2} \qquad \textbf{3.4}$$

where $\sigma_{ys}$is the yield strength of the material.

3.2.3.Crack resistance

The supposition that the straining energy is accessible for superficial energy of novel fissure appearances does not smear for flexible solids whereas rest of the energy extravagant tools are existent. For instance, in glassy solids, significant energy is disbursed during the crusade of displacements in the crystal framework and this materializes at functional stress that is fine under the critical strength of the material. Disruption measure in a ductile material is a signal of yield or plastic distortion, or plastic course.

Griffith's equation was improved by Irwin and Orowan [32] that considered the non-reversible energy contrivances related with the plastic zone. The modified equation is expressed as:

$$\frac{dU_s}{dc} = \frac{dU_\gamma}{dc} + \frac{dU_p}{dc} \qquad \textbf{3.5}$$

The right side of the equation is called crack resistance and is represented by$R$. Ductile materials are harder than frail materials as they can captivate energy in the plastic region. In contrast to it, brittle materials can only disperse stowed elastic strain energy by superficial space creation method.

3.2.4.K_{1C}, the Critical Value of K_1

The stress intensity factor K_1 is called as a "scale factor" that exemplifies the extent of the stress at various coordinates (r, θ) nearby the crack tip. When apiece one of two cracks in two dissimilar samples are encumbered such that $K_1$is identical in respectively sample, then the level of the stresses in the neighborhood of every crack is specifically alike. If the functional stresses are increased, keeping the same value of $K1$ in each specimen, then eventually the energy balance criterion will be satisfied and the crack in each will extend. K_{1C}Outlines the beginning of crack propagation. It does not certainly specify breakage in the specimen. This is linked with the crack solidity. It is generally considered as a solid asset and can be utilized to illustrate strength. In contrast, its resolve is not only contingent on particular data of actions inside the plastic district. Reliable and reproducible numbers of K_{1C}ismerely obtainable when cases are verified in planar strain. In planar stress, the acute value of K_1 for fracture hinges on the width of the plate. Henceforth, $K_{1C}$is frequently named as "plane strain fracture toughness". Lower values of K_{1C}shows that, for a specified stress, a material can lonely endure a minor length of crack beforehand a crack outspreads. The condition $K_1 = K_{1C}$does not essentially resemble fracture of the sample. K_{1C}Defines the commencement of crack spread. No matter it is a steady or unbalanced state depends upon the crack system. Disastrous rupture transpires once the equipoise state is uneven. For cracks in brittle materials originated by interaction stresses, the crack might be primarily unsteady and turn out to be stable afterwards due to the abruptly fading stress ground.

3.2.5.Equivalence of $G$and K

Let G be defined as being equal to the strain energy release rate *per crack tip* and given by the left-hand side of Eq. 2.3d, that is, for a double-ended crack within an infinite solid, the rate of release in strain energy per crack tip is:

$$G = \frac{\pi\sigma^2 c}{E} \qquad \textbf{3.6}$$

Thus, substituting Eq. 3.3 into Eq. 3.6, we have:

$$G = \frac{K_I^2}{E} \qquad \textbf{3.7}$$

Provided that$K_1 = K_{1C}$, G_c is the critical value of strain energy release rate in sense of the material that tips to crack extension lead and perhaps breakage of the sampling. The association concerningK_1 and G is noteworthy since it incomes thatK_{1C}circumstance is an obligatory and adequate principle when crack progression is undergone as it symbolizes the stress and energy equilibrium standards.K_{1C}defines the indirect stresses at the tip of the crack accompanied with strain energy discharge ratio at the inception of crack allowance.

3.3. Fatigue Rate Curve

The Fatigue Crack Growth rate curve is a $da\ /\ dN$versus ΔK curve as shown in figure 3.5. The graph curve is usually divided into three regions. i.e. Region I, II and III. In region I, the early crack rate development is represented. In this region, FCG rate is in the range of $10^{-6}\ mm/cycle$ or indeed, even short of what it is. This locale is astoundingly touchy to littler scale structure features. For instance, grain size, the means stress of the associated load, the atmosphere and the working temperature. The critical area in this region is Fatigue Crack Growth (FCG) verge, ΔK_{th}. This is the specific point where fatigue crack propagation starts. For areas of the specimen where Stress Intensity Factor (SIF) are below this range, crack will not propagate.

Region II is termed as the intermediary region. In this zone, the growth rate is in the range of 10^{6}-10^{3} mm/cycle. Crack growth is stable throughout this region. Power Equation is applied on the data and the Plastic Zone at the crack tip is large in contrast to the mean grain size. As, Power Equation is applied on the data, the curve developed from the extracted data will follow a linear path on a log-log plot (figure 3.5). Linear Elastic Fracture Mechanics (LEFM) concepts apply here. Mean stresses have the maximum effect on the results in Region II, but this influence is smaller when matched with region I.

The final zone which is region III, starts. In this region, figure 3.5 depicts clearly that the curve again starts inclining. It is generally in the order of 10^{3}mm/cycle and more. This is remembered as extraordinary fatigue crack growth rates that are the results of frequent and unbalanced growth preceding to absolute failure of the specimen.

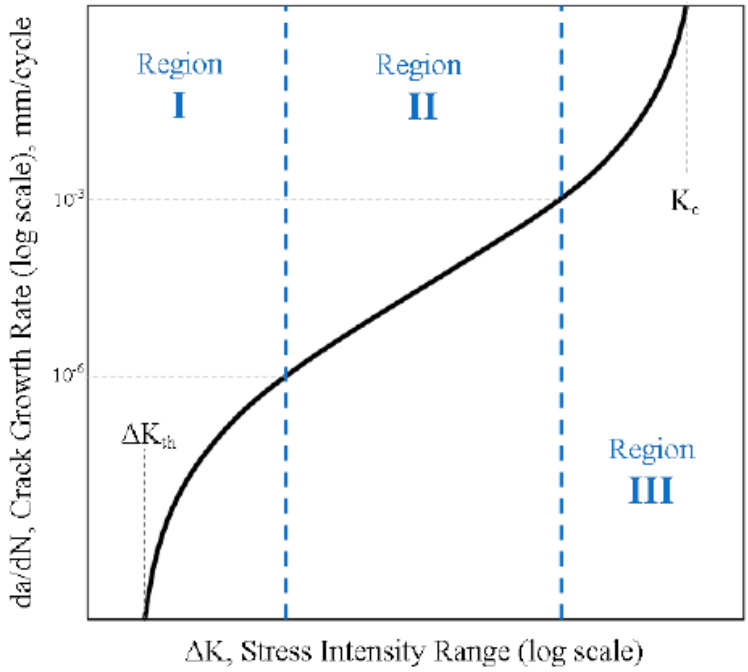

Figure 3.3. Fatigue Crack Growth Rate Curve [2]

3.4. Artificial Neural Networks

There are a number of problems that cannot be dealt with a computer algorithm. Human beings have learning capability which computer processor lacks. The impressive quality of a brain of living things is that they learn on their own accompanied with prior knowledge and information gathered from environment. Computers have a program on which it works depending upon the application. What do we need in computers to replicate brain like capability to decide on their own? The idea is developed from a biological process of transferring information and decision making i.e. neurons. So, an artificial neural network is made to serve the purpose. An example of structure of a neural network is shown in Figure 3.5.

An Artificial Neural Network (ANN) is characterized as a framework created by interconnection of processing components. The data is handled by their dynamic reaction to outside information sources. The learning in design of neural network can be categorized as unsupervised learning or supervised learning. In supervised learning, target flag is given by individual input signals. The point is to diminish the error flag which is the contrast between output flag and target flag through ceaseless adjustment of weights with respect to target flag. In unsupervised learning, signal is arranged with no requirement of target flag.

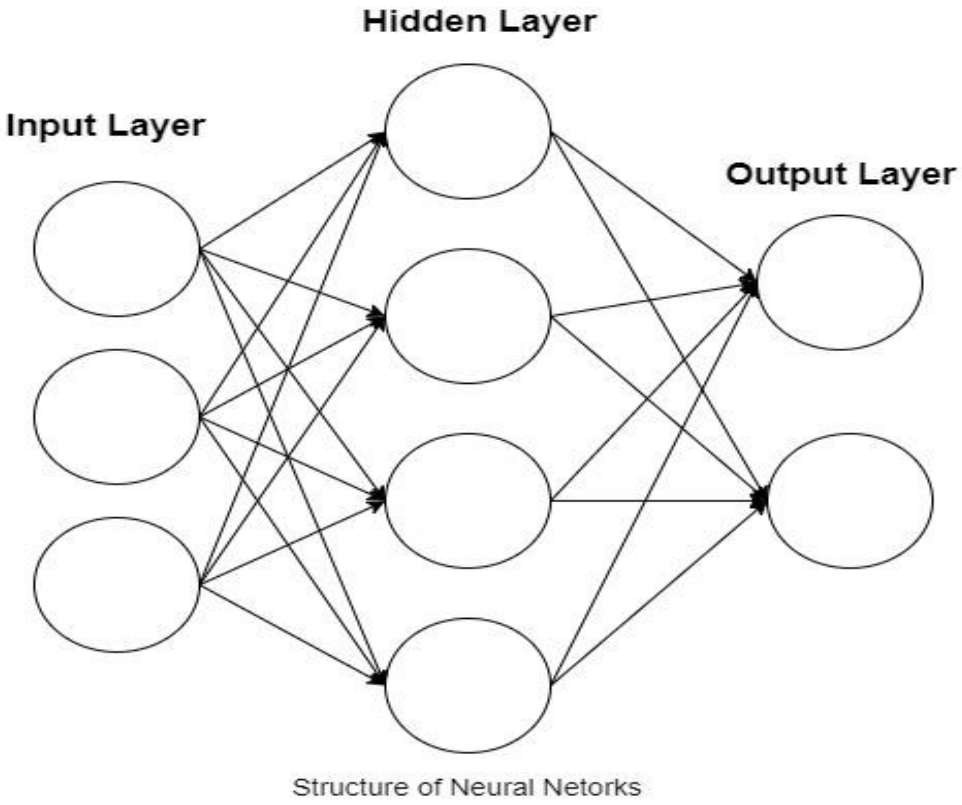

Figure 3.4. Feed Forward Neural Network Structure

To have an enhanced consideration of an Artificial Neural Network, it is required to have an intuition on exactly how CPU works. A PC has a Central Processing Unit that discourses a memory locality somewhere records or instructions are stockpiled contingent upon the program. The processing element execute an action and outcomes are stowed in a definite memory location conferring to the necessity. In this computational structure, commands are chronological or coherent and a state of a certain variable is liable to be traced from process to process. In divergence to serial computers, ANN's working is not chronological or deterministic. These networks do not implement program instructions. Instead they reply to the evidence cradle delivered as they arise. Furthermore, re organized gen is kept in instigation "state" of the structure as an alternative of loading it in the isolated memory location like serial CPUs. ANN is concisely explicated as follows.

An Artificial Neural Network (ANN) is characterized as a framework created by interconnection of processing components. The data is handled by their dynamic reaction to outside information sources. The motivation comes from biological neural networks. ANN's may include a hardware computing device or an algorithm that are modeled after observing a neuronal structure of mammals but on a much smaller scale obviously. Some larger networks contain hundreds or thousands of connections and processing units but a biological neural network contains billions of neurons. An Artificial Neural Network is structured in the form of layers. The layers consist of nodes interconnected with each other which are powered by an Activation Function. The pattern of the systems is presented to the network by an input layer which communicates to one or more hidden layers for processing. Hidden layers possess weighted functions which is the actual driving force of processing. After processing, hidden layers involved in the process communicate to the output layers where information is transferred as output of the network. An ANN has the learning rule which continuously modifies the weights of the connections according to the input presented. So, the basic components of a network come out to be as follows

- Neurons
- Connection and Weights
- Propagation Function
- Learning Rule

Many kinds of ANN are utilized to forecast the output. These methods embrace an ANN accompanied with supervised learning and optimization algorithms.

Neural networks are computational representations that are biologically stimulated from anthropological intelligence. These networks involve neurons inter-connecting distinct processing elements. Data is served from the structure to a neuron by means of some conduits called dendrites. This data or effort is now augmented through magnification element well-known as synapses or weights and is summed collected by the handling unit. Then the biased addition is furthermore treated by the neuron which comprehends an activation function that accepts the weighted sum and harvests an output subjected to its prototype. The activation function is of somewhat customary method liable on the category and neural network structural design. Grounded on the learning models, neural network design can be categorized into two classes. The two learning prototypes are supervised and

unsupervised learning. In the supervised method of learning, the mandatory or anticipated output of neurons are in use as a target to sequence the neural network for the use of grouping commitments. On the other side, in the unsupervised learning the anticipated 'target' in contradiction of an input is unfamiliar and information is bunched into diverse courses founded on likeness. In this regard hill climbing, genetic algorithms, simulated annealing, and particle swarm optimization are some of the examples of supervised learning.

There are three layers in the structural design of feed forward neural network. Let us consider an input layer$i$, a hidden layer h and an output layer o. The learning data is given by:

$$\varphi = \{(X_o, Y_o)\}_{o=1}^{E} \qquad \textbf{3.8}$$

This is acquired from space arrangement where each sample relates an input vector $X_o \in \mathbb{R}_n$ and$Y_o \in \mathbb{R}_p$, where $Y_o$is the wanted vector reaction to an input X_o. Neurons numeral at the input level are similar as the input topographies figures whereas output layer neurons hinge on output classes. There is no such rule for the selection of hidden layer number of neuron. The hidden layer neurons are random and can be nominated on the subject of the concern of ANN.

The constraint of vector$I_n = [i_1, \quad i_2, \quad i_3, \quad , \dots, \quad i_n]$, is specified to a network as input layers that in reaction proliferate in the hidden layers by weights t_{io}. A vector $b = [b_1, \quad b_2, \quad b_3, \quad , \dots, \quad , b_n]^T$ with '1' as input is added to respective hidden layer neuron and this vector is termed as ANN weight.

$$y = \sum t_{io} i_i + b \qquad \textbf{3.9}$$

Here, $y = [y_1, \quad y_2, \quad y_3, \quad , \dots, \quad , y_n]^T$

Where y_i is the output sum alongside the input accessible in the input layer.$t_{io}$is the biasamongst the input and hidden layer.$i_i$is input feature vector, and $b$is the partiality vector.

The output value of hidden layer neuron is resolute by the activation function, given by equation 3.10, is added to y that is attained by equation 3.9

$$P(y) = \frac{1}{1+e^{-y}} - 1 \quad \textbf{3.10}$$

Where $P(y)$ is the sum of output in contrast to the input layer.

The activation function of output deceits between the range of $[0, 1]$and is multiplied by new biasesm_{jk} for its scheming and nourished to output layer following afore cited route. The bias of feed forward neural network gets itself updated depending upon Mean Square Error (MSE) which is given by

$$MSE = \frac{1}{N}\sum_{i=1}^{N}(\partial(l_i; \boldsymbol{x}) - O_i)^2 \quad \textbf{3.11}$$

Where $\partial(l_i; \boldsymbol{x})$ the output objective of input vector, and $O_i$is output of neural network.

The neural network weights are updated for each input vector as given by equation 3.4

$$W_o = W_{o-1} + \Delta W_o \quad \textbf{3.12}$$

Generally, when we talk about optimization of Artificial Neural Networks the main concern is objective function which is the mean square error function. The aim is to optimize the values of weighted connections in order to minimize mean square error i.e. objective function. The following is a brief introduction of the optimization techniques used in this paper.

3.4.1.Genetic Algorithm based Optimized Neural Network

Genetic algorithms are like stochastic beam searches, but each new element of the population is a combination of several offspring's. In particular, genetic algorithms select pairs of off springs to create a new one, some value for the variable taken from an own parent, and the rest of the values from other parent, loosely analog DNA in split's sexual reproduction.

The new operation found in genetic algorithms is called crossover. Crossover uniformly selects two offspring and creates two new offspring, called the children. The child value for each offspring comes from their respective parents. A one-point cross over is common method of crossover in order of assumed variables. An index *i* is randomly selected. One of the children is constructing by selecting the variables values before *i* from one parents,

and the variables values after *i* from the other. Another child takes other values. The efficiency crossover depends on the total position of variables. Order the variables are part of the design of genetic algorithm.

For hard, non-linear capacities Genetic Algorithm has been performing exceptionally well in acquiring worldwide arrangements. Fundamentally, a goal, for example, minimization of the sum of squared errors or total of absolute errors, is decided for optimizing the neural system. Having a benefit of selected goal point, each candidate acquires attention to the fundamental population of randomly selected initial points are used for analyzing the goal position. The mentioned characteristics are then used as a part of assigning chances for each of the emphases that are included in the population set. To achieve minimization, that is the case of sum of squared errors, the point having the lowest objective function is assigned the highest probability. When each point is assigned its respective probability, a new population of points is drawn from the present population as a replacement. The points are picked arbitrarily with the probability of acceptance, equal to a probability value that is allotted to it. Therefore, the points with minimum sum of squared errors are most favorites to be represented in the new population. The points consisting a new population are then arbitrarily made in pairs for crossover. Each point is represented as a string of n different weights. A position along a string is arbitrarily selected for sole set of points and previous constraints are swapped between these points. Each crossover gives a new point having constraints from both parent points. As a result, each weight has much less chance of being replaced with a value arbitrarily selected from the parameter space. This is called mutation. Mutation augments the Genetic Algorithm by occasionally inserting a random point for a better search of whole parameter space. In this way the Genetic Algorithm is permitted to escape from local optima provided the new generated point proves to be a better solution than those that have been previously found better. This provides a more robust solution. Thus, resulting set of points becomes the new population, and the cycle repeats until a best solution converges.

As, this method seeks in numerous ways at times, the chance to discover a globally ideal increments. The arithmetic's comparability to regular choice inspires its name. As the

Genetic Algorithm moves forward through ages, the superlative parameters to optimize the target capacity will repeat in finding who and what is to come, while the parameters that are ineffective comparatively vanish in survival of the best solution.

Let us assume that we have"a" individuals population (a = even). The genetic algorithm works by upholding the discrete value of "a" as a cohort and utilizes these discrete values for new cohort via the following steps:

- Randomly selected pairs of individuals who have a greater chance of being selected as an assembler of individuals. How often choose a capable individual as an individual less suitable depends on the difference in fitness levels and the temperature parameter.
- For every pair, carry out a crossover.
- Randomly mutate a few values selecting by other values for a few randomly selected variables. This is a random walk step.
- The algorithm proceeds in this pattern until it has produced a individuals, and after this the process proceeds to the next generation.

Following is a pseudo code, explaining the algorithm

```
Test Set P = ø
for Condition C
do
search Start point Sn
     repeat
          for (a = 0; a < |Sn|/2; a++)
          do
          select randomly two parents from population
          reproduce two children by crossover operation
          insert children into new generated list
               if children satisfy the condition C
               P = P ∪ { Σ of new children}
               break
```

```
                end
            end
        continue mutation and add the children into
generation list
        until Condition C is satisfied or maximum iteration
is reached
end
```

3.4.2.Simulated Annealing based Optimized Neural Network

Annealing is a method in metallurgy where metals are gradually cooled to make the metal temperature reach at low energy state. Simulated annealing is used for optimization. Simulated annealing is a method of reducing temperature gradually; initializing a group of random search at higher temperature ultimately becoming pure greedy descent as temperature reaches toward zero. At local minima the randomness should try to leap out in search of area which has low heuristic; greedy descent will lead to local minima. Occurring of worse steps at high temperatures is more likely than at low temperatures.

Simulated annealing keeps the present values of variables. At each step, it takes random variable by assigning a value to that random variable. If the value assigned to the random variable is shown any increase then previous one, the algorithm accepts the new value and then the new value is now present value. Otherwise, it keeps the previous value with a number of probability, depends upon the temperature and the present value how much bad it is. If the change in the value is not acknowledged, the present value is remaining same. Simulated Annealing is a probabilistic search which look for a single suitable solution. It takes its concept form the process of annealing in the field of metallurgy. Annealing is a process where metals are heating above their melting points, hold and then cooled slowly to solidified form attaining minimum energy configuration in order to get a perfect crystalline molecular structure. The purpose is to find a global minimum when various

algorithms stuck in local minima. The innermost loop of this algorithm runs same as of hill climbing but the difference between these two is that it searches for random move instead of best move. If that move is better than current, it is updated otherwise the algorithm searches for another one. Following is the flowchart of the simulated annealing process

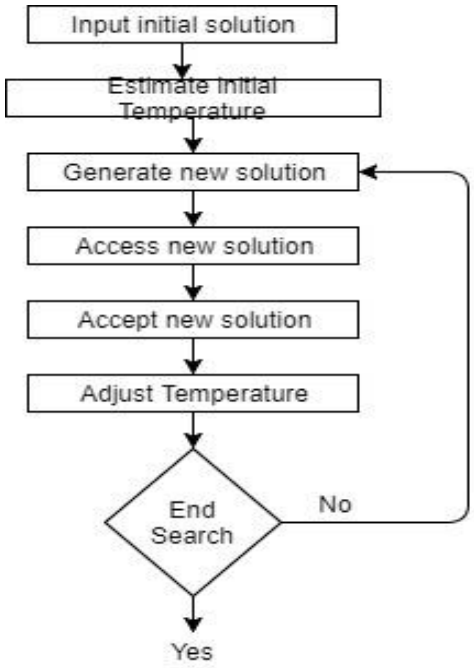

Figure 3.5. Flowchart of Simulated Annealing Optimized Neural Network Algorithm

For controlling the bad steps, there is a positive value of temperature T. let's assume x is the present value to each variable. Assume that $f(x)$ is the assessment of value x to be limited. Overcoming the challenges, f is usually the number of conflicts. Simulated annealing is chosen by random neighbors, which give us a new value x'. If $f(x') \leq f(x)$ and it accept that value the value becomes a new one. Otherwise, the value is randomly accepted only by the probability $e^{(f(x)-f(x'))/T}$. Therefore, if $f(x')$ is near to $f(x)$, the value is accepted probably. The value of exponent is approaches to zero if the value of temperature is high, for this the probability will be 1. The value of exponent is approaches to $-\infty$ if the value of temperature is 0, for this the probability will be 0.

Table 3-1: Probability of simulated annealing accepting worsening steps

Temperature	Probability of occurrences		
	1-worse	**2-worse**	**3-worse**
10	0.9	0.82	0.74
1	0.37	0.14	0.05
0.25	0.018	0.0003	0.000006
0.1	0.00005	2×10^{-9}	9×10^{-14}

Table 3-1. shows at different temperature the occurrence of probability of worse steps. In this Table, *R*-worse means that $f(x')-f(x)=R$. Form the table, the value of temperature T is 10, the probability of acceptance for the change in 1-worse is $e^{-0.1}$ approx. *0.9*; the probability of acceptance for the change in 2-worse $e^{-0.2}$ approx. *0.82;* the probability of acceptance for the change in 3-worse $e^{-0.3}$ approx. *0.74*. The value of temperature T is 1, the probability of acceptance for the change in 1-worse is e^{-1} approx. *0.37*; the probability of acceptance for the change in 2-worse e^{-2} approx. *0.14;* the probability of acceptance for the change in 3-worse e^{3} approx. *0.05*. The value of temperature T is .1, the probability of acceptance for the change in 1-worse is approx. *0.0005*; the probability of acceptance for the change in 2-worse e^{20} approx. $2x\ 10^{-9}$*;* the probability of acceptance for the change in 3-worse e^{30} approx. $9x\ 10^{-14}$. The temperature at T .1 the probability .0005, it is basically only steps that increase the value or leave it unchanged.

At higher temperature, T = 10, the algorithm try to accept the steps that only worsen a small amount; It does not aim to accept very big bad steps. There are several benefits to upgrading steps. As soon as the temperature T = 1, bad feet, although they may be not as much expected. When the temperature T = .1 there is very less chance of opening the wrong choice.

Simulated annealing requires a schedule of annealing, which determines about the changes in temperature as the search is done. The common arrangement of cooling is geometric cooling. An example of geometric cooling arrangement starts at a temperature T = 10 by multiplying 0.97 for each step; the value of temperature will be 0.48 to 100 steps.

Following is the pseudo code for Simulated Annealing Optimized Neural Network Algorithm

```
function ANNEALING-SIMULATED-(prob.statement, plan)
return answer state
inputs: prob.statement
plan: "time" required to reach "temperature" plotting
     m_current←NODULE-MAKING-(prob.statement.STARTING-
CONDITION)
LOOP (for)t = 1 to∞do
     T ←plan(t )
if T = 0 then return m_current
     m_next←anarbitrarilydesignatedreplacement value of m_current
ΔE ←m_next.VALUE – m_current.VALUE
if ΔE >0
     m_current=m_next
else
     m_current=m_next with probable valuee^(ΔE/T)
end
```

3.4.3. Hill Climbing based Optimized Neural Network

Hill climbing is a process used to belong to the optimization group locally searching. This algorithm is quite simple to implement; this is the first alternative to the problem. In some

cases, hill climbing shows better results, otherwise many advanced search algorithms are present which shows better results. Hill climbing algorithm is used for solving those problems that have several solutions, some of them is superior to others. It starts from the initialization of random solution and making some changed in the solution after every iteration little improvement observes. If the algorithm does not observe any improvement, it ends. At the time of termination, the existing solution is near to the optimal, but it cannot guarantee that the solution is an optimal solution this is the drawback of hill climbing.

For example, hill climbing algorithm may be applied to the problem of travelling salesman. It is very easy for finding the solution to visit all towns, but it result is satisfactory related to the accurate solution. The hill climbing algorithm begins with some solution and minor improvements that are changing the order in which two towns visit. In the end, he gets a lot better route. Earlier climbing was widely used in artificial intelligence, reaching the objective situation to start a node. The choice of the coming node and the initial node can be changed in accordance with the attached algorithm list. The algorithm tries to increase (or decrease) the function f (y), where y is the discrete conditions. These conditions are usually presented in vertical graph, where sides of graphics are proximity coding or graphical similarities.

Hill climbing tries to adapt the graph value from peak to peak, in order increase or decrease the function value locally, even after a local maxima or minima is reached. Hill climb can operate in a continuous space, in this case, the hill climbing is called gradient ascent. In hill climbing problems: local maxima (we climbed to the top of the hill and lost on the mountain), plateau (all around us is as good as I), and ridges (we are on the ridges but we cannot directly application operator to improve our situation, so we have the application of more than one operator to get there). Solutions are, make big jumps (to handle plateau or poor local maxima), apply more rules to the test.

Hill climbing suited best for problems where heuristic improves gradually as quickly as possible to get a solution. It works badly, which has sharp drops. It is assumed that local improvement leads to a global improvement

Hill climbing is a type of an optimization techniques in artificial intelligence is very useful in solving the problems with complex hierarchy. It always keeps itself busy in monitoring current state and future state and tends to improve the current state with the help of an evaluation function while performing iterations. Basically, it is seen as a loop that continuously keep on moving towards the increasing value and terminates when highest peak is met. i.e. no neighbor is around with the higher value. The loop is run in a way that best known solution at the present stage $m_{current}$ is reproduced in the form of an offspring $m_{neighbor}$. If the reproduced offspring $m_{neighbor}$ is better in value than $m_{current}$, it is updated and becomes $m_{current}$, otherwise it is neglected and cycle continues to search for a new solution or cessation condition. It is a local search algorithm that only looks for its immediate neighbors. Following is the pseudo code for the presented algorithm.

```
function CLIMB-HILL-(question)
     return a state that is a local maximum
          inputs: question
           state: m_current, m_neighbor, nodule
          m_current←NODULE-MAKING-question.STARTING-CONDITION)
     LOOP-(for) do
          m_neighbor←a number with highestreplacement of m_current
     if m_neighbor≤m_current
     in case
     return m_current.STATE
          m_current= m_neighbor
end
```

3.5. Proposed Technique

In Fig. 3.7, 3.8& 3.9 the proposed methodology is explained by making the use of flowcharts. Firstly, a two input and a single output data is extracted from the literature. In the proposed methodologyΔK and R are engaged as input and da/dN as output. After that the experimental data is prepared and processed in order to make it able to be used in the MLA's. in this process, uncooked tentative statistics that include SIF range, ΔK andthe load ratio, R while FCG rate,da/dN occupied as output. These statistics are assimilated from preceding benchmark literature. The developed data need to be carefully chosen and pre-processed beforehand it must be used in the algorithms that are proposed in the technique. The data is separated keen on training and testing groups. The learning algorithms are trained for thorough going re iterations by means of training set of data up until a stipulated Mean Square Error (MSE) is attained or maximum reiterations are executed. After reaching prerequisite worth of MSE or administering all-out recapitulations. The undertaken network is trained and the weighted connections are halted. This taught ANNs are tested to realize which of the proposed algorithms outbursts the non-linearity in the Paris region in the best way during FCG rate calculation. Fig. 3.6 shows the flowchart of well-trained artificial neural network. During this process, after the above mentioned data pre-processing, ANN is established for training. After completion of training, network is compared with experimental data in order to check the accuracy. After comparison parameters are tuned for optimization of ANN.

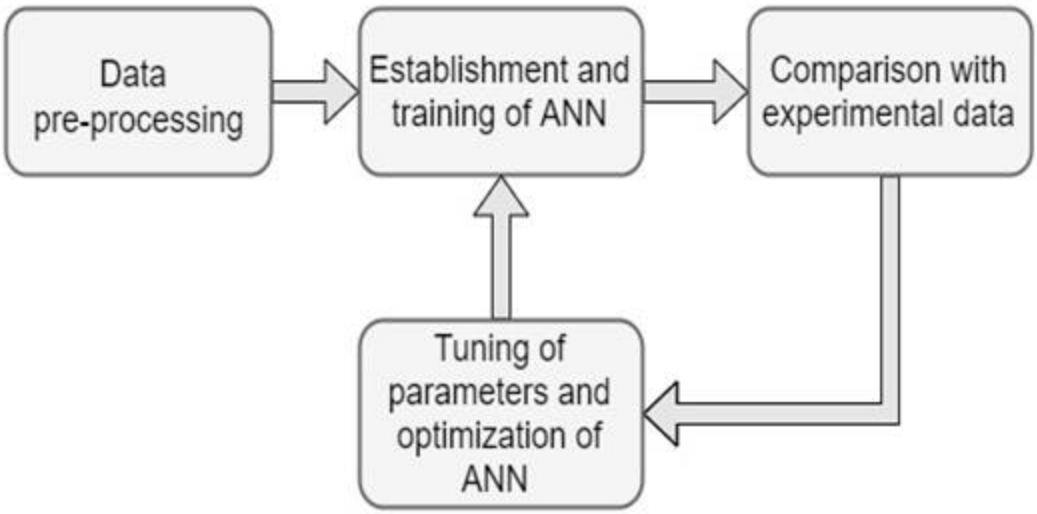

Figure 3.6. Flowchart of trained ANN

For accurate prediction of FCG rate, proposed technique presents a relative study after execution of different regression based optimized MLAs which include Genetic Algorithm based Optimized Neural Network, Hill Climbing based Optimized Neural Network and Simulated Annealing based Optimized Neural Network.

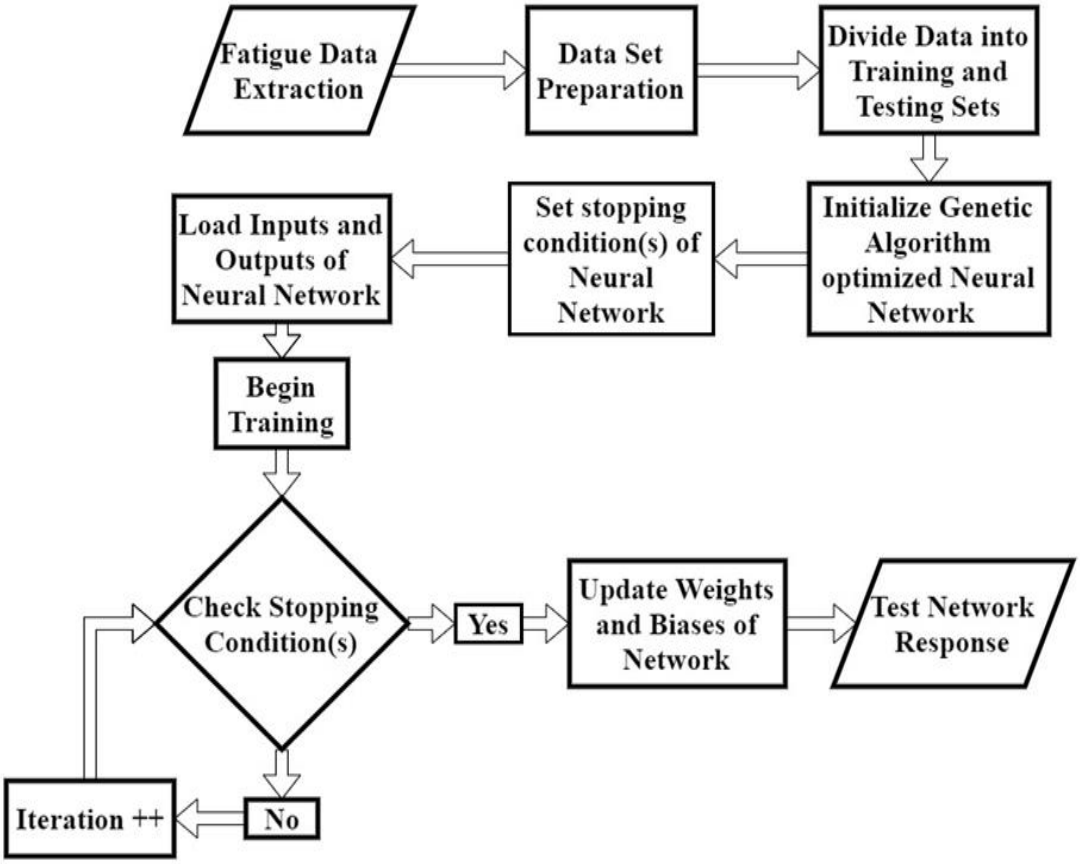

Figure 3.7. Flow Chart of Genetic Algorithm based Optimized Neural Network

Figure 3.8 represents the flow chart of the proposed technique with Genetic Algorithm Optimized Neural Network used as a regression tool here. Flow chart presents that after data extraction, it is prepared and divided into different groups of training and testing data sets followed by initialization of algorithm. Inputs and outputs are fed to the network after analyzing stopping conditions of neural network. During the training process stopping conditions are continuously checked. If any of them is achieved, updated weights and biases are nurtured to the network at which network response is tested.

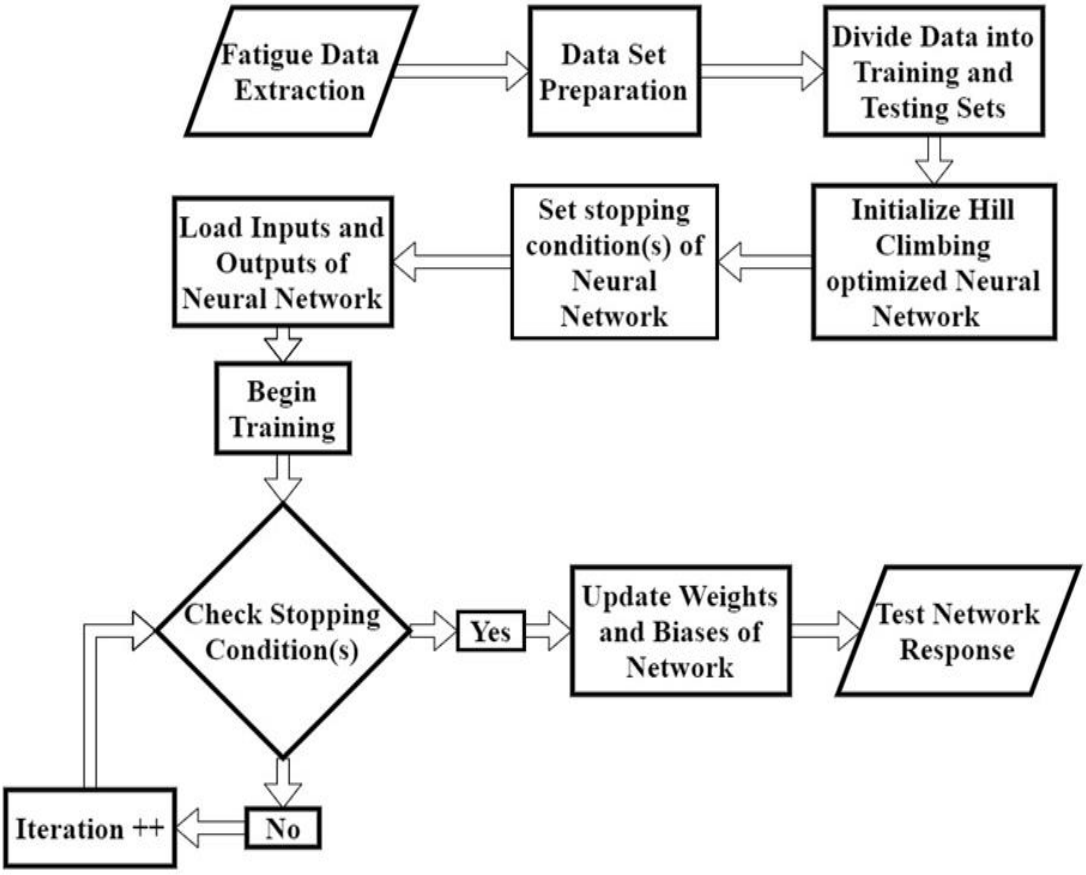

Figure 3.8. Flow chart of Flow Chart of Hill Climbing based Optimized Neural Network

Figure 3.9 represents the flow chart of the proposed technique with Genetic Algorithm Optimized Neural Network used as a regression tool here. Flow chart presents that after data extraction, it is prepared and divided into different groups of training and testing data sets followed by initialization of algorithm. Inputs and outputs are fed to the network after analyzing stopping conditions of neural network. During the training process stopping conditions are continuously checked. If any of them is achieved, updated weights and biases are nurtured to the network at which network response is tested.

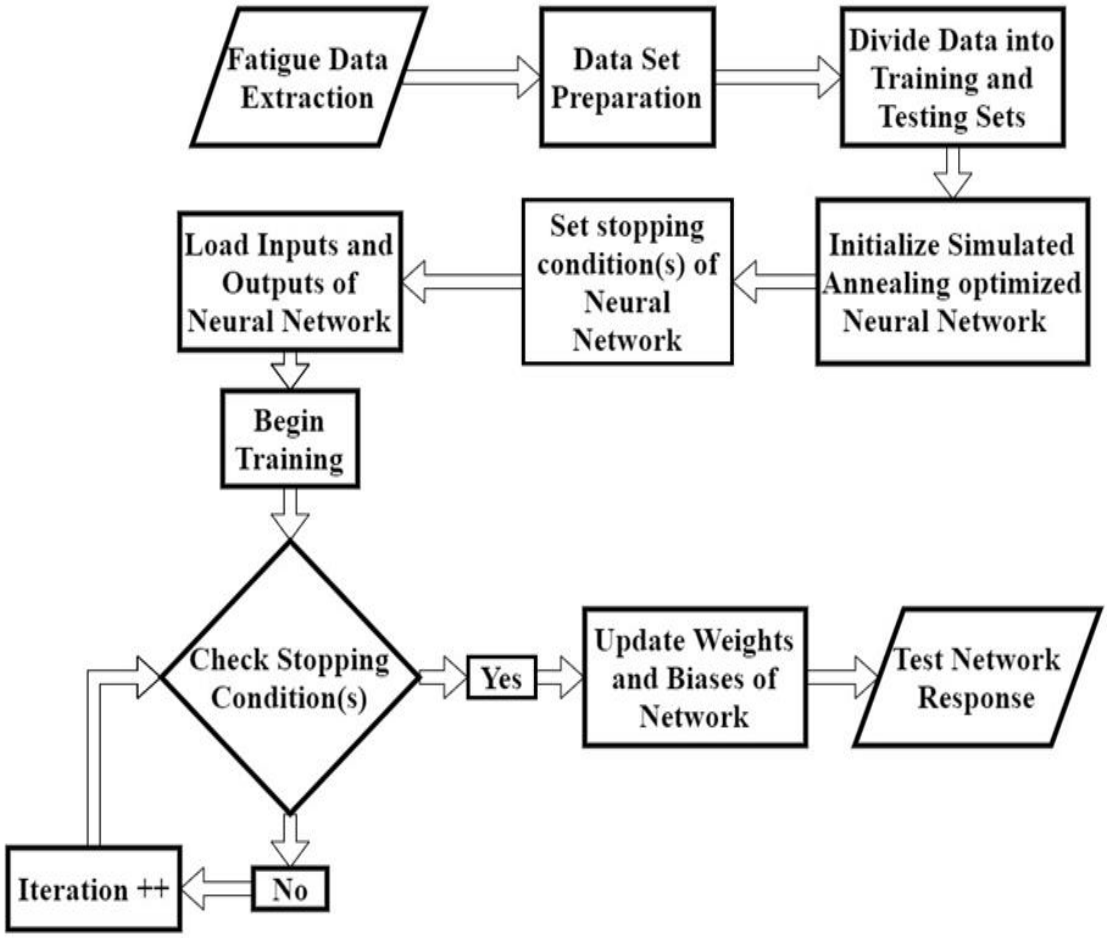

Figure 3.9. Flow chart of Flow Chart of Simulated Annealing Optimized Neural Network

Figure 3.10 represents the flow chart of the proposed technique with Genetic Algorithm Optimized Neural Network used as a regression tool here. Flow chart presents that after data extraction, it is prepared and divided into different groups of training and testing data sets followed by initialization of algorithm. Inputs and outputs are fed to the network after analyzing stopping conditions of neural network. During the training process stopping conditions are continuously checked. If any of them is achieved, updated weights and biases are nurtured to the network at which network response is tested.

3.6. Summary

The discussion in this chapter can be summarized as given in the following lines

- This chapter describes the techniques used to accomplish the ranges of thesis as well as the background theory linked to them
- Fracture mechanics is mainly categorized as Linear Elastic Fracture Mechanics (LEFM) and Elasto-Plastic Fracture Mechanics (EPFM). LEFM gives tremendous results for brittle-elastic materials that include high-strength steel, glass, ice, concrete, etc. On the other hand, plasticity will always go before fracture for ductile materials.
- The FCG rate curve is a da/dN versus ΔK curve. The curve is divided into three regions. The critical area in this region is Fatigue Crack Growth (FCG), ΔK_{th}. This is the specific point where fatigue crack propagation starts. For areas of the specimen where Stress Intensity Factor (SIF) are below this range, crack will not propagate
- An ANN is characterized as a framework created by interconnection of processing components. The data is handled by their dynamic reaction to outside information sources. The learning in design of neural network can be categorized as unsupervised learning or supervised learning.
- Genetic algorithms are like stochastic beam searches, but each new element of the population is a combination of several offspring's. In particular, genetic algorithms select pairs of off-springs to create a new one, some value for the variable taken from an own parent, and the rest of the values from other parent
- Simulated annealing keeps the present values of variables. At each step, it takes random variable by assigning a value to that random variable. If the value assigned to the random variable is shown any increase then previous one, the algorithm accepts the new value and then the new value is now present value. Otherwise, it keeps the previous value with a number of probability, depends upon the temperature and the present value how much bad it is. If the change in the value is not acknowledged, the present value is remaining same.

- Hill climbing is a type of an optimization techniques in artificial intelligence the is very useful in solving the problems with complex hierarchy. It always keeps itself busy in monitoring current state and future state and tends to improve the current state with the help of an evaluation function while performing iterations
- Flow charts of algorithms used in the proposed technique are presented. The presented technique includes the data extraction process followed by data set preparation with the help of regression based machine learning algorithms by elaborating all the necessary steps required to initialize, train and test the network.

4. EXPERIMENTATION

This chapter provides the detail of experimentation setup carried out to acquire the desired data in order to implement the proposed technique. Different test conditions and module specifications are explained with the help of tables and figures.

4.1. Experimentation Setup

The extraction of data on which experimentation is to be carried out is the courtesy of Fracture Technology Associates Laboratory which is a profitable, autonomous laboratory providing specimen testing facilities for about 40 years. The owner of the laboratory is J. Keith Donald who is universally renowned professional with above 40 years' capability in the arena of tentative fracture mechanics. Having trivial but devoted workforce, FTA offers testing facilities and personalized software schemes that is offered to a widespread assortment of private and governmental clients, together with prominent industrialists of airplanes or aerospace materials; purveyors to the transport and grounded automobile engineering sector; manufacturers of dedicated metals including energy industry. Experiments were directed on a servo-controlled, hydraulically-actuated, closed-loop machine-driven testing mechanism which is interacted with a devoted PC for statistics acquirement besides adjusting the factors. Strain gauge based transducers provide the assistance in calculation the displacement. Servo-hydraulic system for static and low frequency dynamic tests on building materials under control of Load/Stress, Displacement Strain.

Perfect both for customary checks, such as compression and flexure on concrete, cement, mortar, blocks etc. and cyclic tests for the determination of secant elastic modulus (E) according to all relevant international standards, and also for measuring, for example, the ductility and fracture energy of concrete reinforced with fibres (FRC) and lined with polymers (FRP), or the toughness of sprayed concrete slabs (shotcrete) under concentrated load tests. The console is connectable to up to four test frames. Servo Hydraulic Control Console is shown in Figure 4.1. Its Specifications are as follows:

Hydraulic Group

- Max. working pressure: 700 bar
- Hydraulic ports to test frames: 4
- ON/OFF electronic valves: 4

Hardware Firmware

- Extreme Resolution: 1/524,000 divs
- Input stations: 8
    - For load sensors: 4
    - For displacement transducers: 4
    - The formation can be changed by the operator for particular requirements excluding the load sensors

Physical specifications

- Power rating: 750 W
- Voltage: 230V, 50 Hz, 1 ph, 230 V, 60 Hz, 1 ph and 110 V, 60 Hz, 1 ph
- Dimensions (lxwxh): 470x410x1000 mm
- Approximate Weight: 120 kg, apart from personal computer and printer

Figure 4.1. Servo Motor Control Console for Testing of Materials [32]

2324-T39 Aluminum Alloy is an advanced strength, concentration meticulous composition form of 2024-T351 of alloy 2024. It was established for the materials that are subjugated by tension, fatigue and fracture critical plate uses. The T39 addition, settled over distinctive formulating rehearses, rallies together strength accompanied with fracture toughness possessions above 2024 alloy specimen. 2324-T39 alloy specimen is applied on inferior wing and central wing package mechanisms of marketable airplane. Physical properties of this alloy are as mentioned below.

Table 4-1: The Useful properties for 2324-T39 Aluminum Alloy [32]

Physical Properties (Metric Units)	
Density ($\boldsymbol{\rho}$)	2.77g/cc
Mechanical Properties (Metric Units)	
UTS	≥470-475 MPa
Tensile Strength at Yield Point	≥365 MPa
Extension at Breaking Point	≥8.0 %
Young's Modulus (E)	72.5 GPa
μ	0.33
Electrical Properties (Metric Units)	
Resistivity (Electric)	$4.5\times10^{-8}\Omega$-m
Thermal Properties (Metric Units)	
Co-efficient of Thermal Expansion (Linear)	23.2×10^{-6} m/m-^{o}C @ 20.0^{o}C 24.7×10^{-6} m/m-^{o}C @ 20.0-300^{o}C
Specific Heat Capacity	0.875 J/g-^{o}C
Thermal Conductivity	151 W/m-K

After processing the raw data acquired from literature for 2324-T39 alloy is plotted using MATLAB 2016 with load ratios ranging between 0.1 and 0.7. The experimental data plot is shown in Figure 4.2.

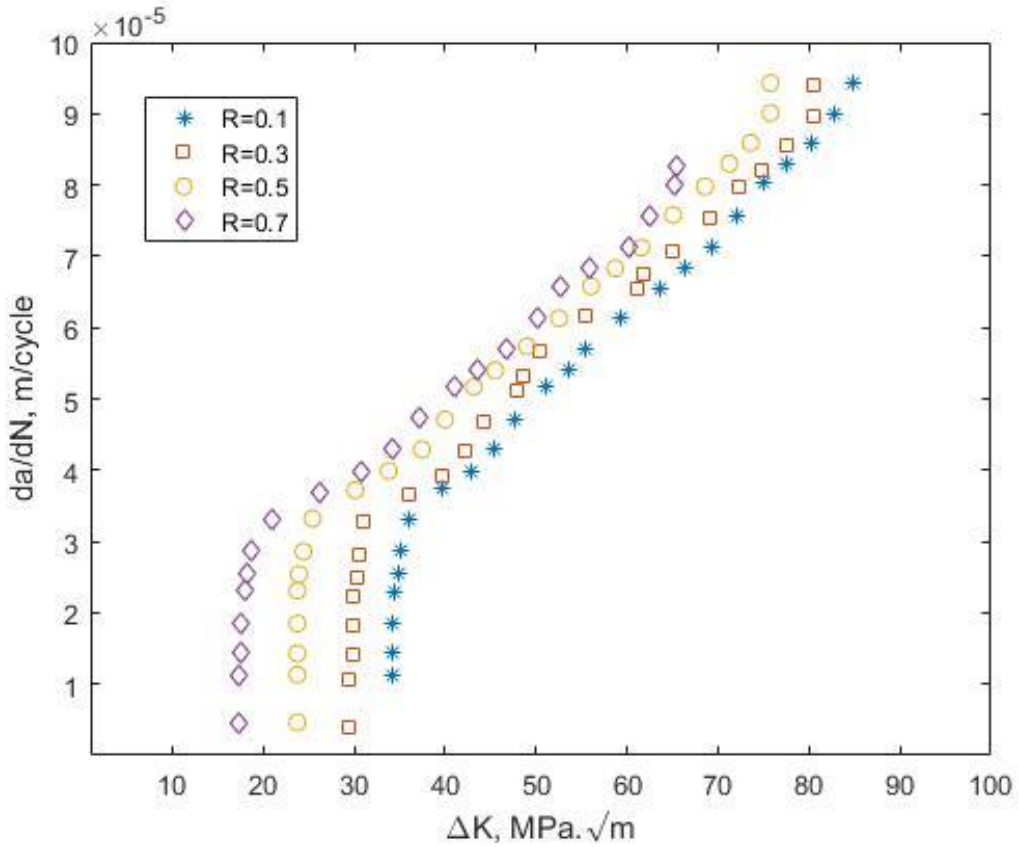

Figure 4.2. Experimental data of Fatigue Crack Growth rate of 2324 T39 Aluminum Alloy

7055-T7511 alloy was explicitly developed to be used in structures subjugated by compression to offer benefits when compared to 7150 alloy in compressive and tensile strengths though upholding various significant material goods including fracture toughness and corrosion resistance. The useful physical properties 7055-T7511 alloy is as given in table 4.2.

Table 4-2: The Useful Properties of 7055-T7511 Aluminum Alloy [32]

Physical Properties (Metric Units)	
Density (ρ)	2.8599×10^{-3} kg/cc
Mechanical Properties (Metric Units)	
UTS	$\geq473\times10^{6}$ Pa
Tensile Strength at Yield Point	$\geq360\times10^{6}$ Pa
Extension at Breaking Point	≥9%
Young's Modulus	7.24×10^{13} Pa
Shear Modulus	2.7×10^{13} Pa
μ	0.33
Electric Properties (Metric Units)	
Resistivity (Electric)	4.90×10^{-8} Ω-m
Thermal Properties (Metric Units)	
Coefficient of Thermal Expansion (Linear)	23.2×10^{-6} m/m-^{0}C @ 293K 24.7×10^{-6} m/m-^{0}C @ 293-593K
Conductivity (Thermal)	150W/m-K

After processing the raw data acquired from literature for 7055-T7511 aluminum alloy is plotted using MATLAB 2016 with load ratios ranging between 0.1 and 0.7. The experimental data plot is shown in Figure 4-3.

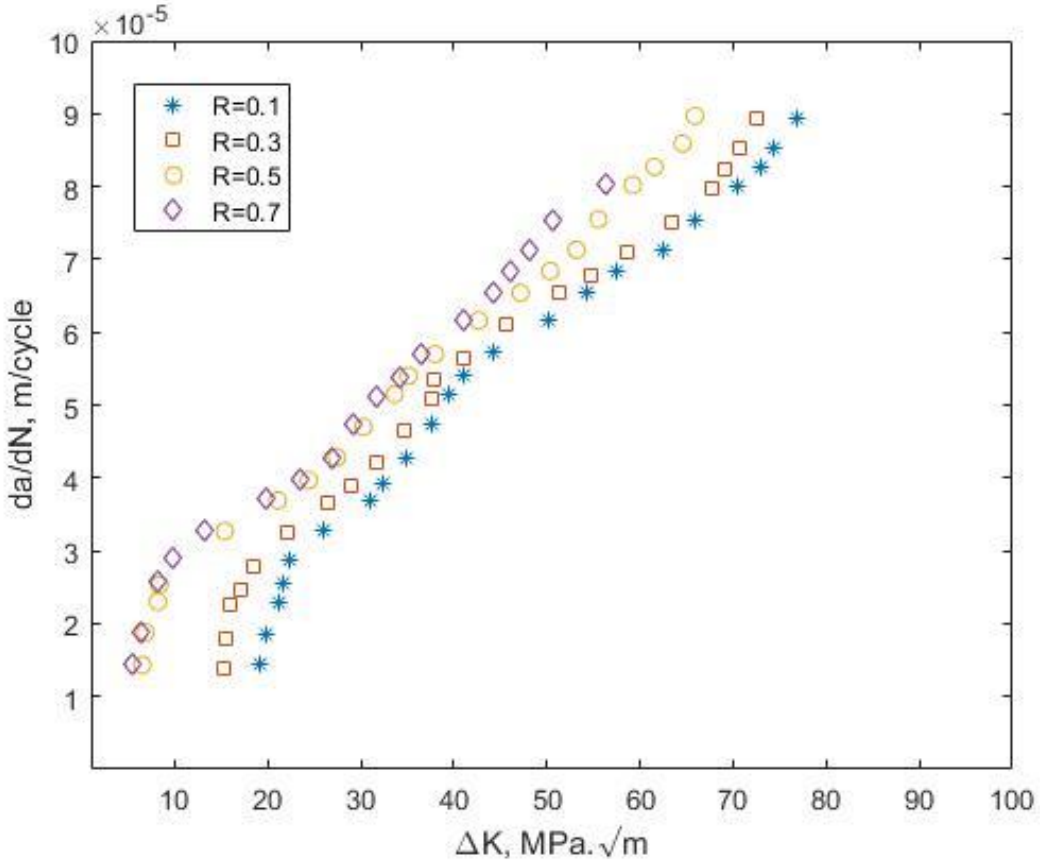

Figure 4.3. Experimental data of Fatigue Crack Growth rate of 7055-T7511 Aluminum Alloy

6013-T651 is generally of extraordinary strength and have excellent resistance to corrosion. It can simply be linked by entire existing welding and brazing techniques. It has outstanding compressive material goods. The uses of this alloy comprise of ABS Braking, hydraulic uses, valves, turbine blades, mechanical parts, weaponries and others. The useful physical, mechanical, electrical and chemical properties are as given in table 4.3.

Table 4-3: The Useful Properties of 6013-T651 Aluminum Alloy [32]

Physical Properties (Metric Units)	
Density ($\boldsymbol{\rho}$)	2.71 g/cc
Mechanical Properties (Metric Units)	
Hardness, Brinell Test	129
Hardness, Knoop Test	162
Hardness, Rockwell 'A' Test	50.5
Hardness, Rockwell 'B' Test	79.5
Hardness, Vickers Test	150
UTS	≥379 MPa
Tensile Strength at Yield Point	≥359 MPa
Extension at Breaking Point	4.5 %
Young's Modulus (E)	6.96×10^{-13} Pa
Machinability	70 %
Shear Strength	248 MPa
Electrical Properties (Metric Units)	
Resistivity (Electric)	4.90×10^{-8} Ω-m
Thermal Properties (Metric Units)	
Coefficient of Thermal Expansion (Linear)	23.4×10^{-6} m/m-^{o}C @ 20.0-100 ^{o}C
Conductivity (Thermal)	164×10^{-2} W/cm-K

After processing the raw data acquired from literature for 6013-T651 aluminum alloy is plotted using MATLAB 2016 with load ratios ranging between 0.1 and 0.7. The experimental data plot is shown in Figure 4.4.

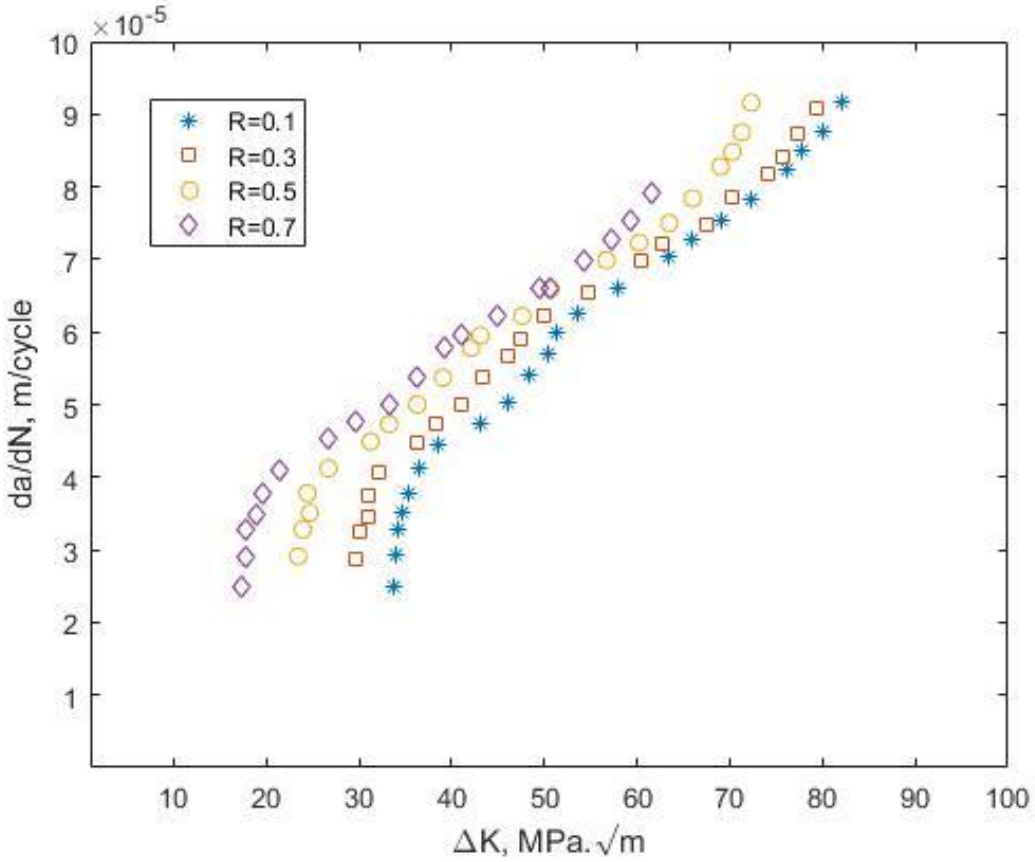

Figure 4.4. Experimental data of Fatigue Crack Growth rate of 6013-T651 Aluminum Alloy

A thumbnail of the experimental conditions to be observed throughout carrying out tests process is as shown in Table 4-4.

Table 4-4: Thumbnail of Experimental Conditions to be observed in the Laboratory

Characteristic of Specimen	**Values**
Thickness (B)	2.2mm-3.1mm (Different for each specimen)
Width (W)	1.016×10^{-5}m
Length of V-cut ($2a_0$)	1.02×10^{-4}m
Alignment	L-T
Testing Frequency	14.9 Hertz
Ambience	Lab midair, 297K, Relative Humidity = 49-56%
da/dN	1×10^{-9} to 1×10^{-1} mm/cycle

4.2. Summary

The chapter can be summarized as follows

- This chapter provides the detail of experimentation setup carried out to acquire the desired data in order to implement the proposed technique

- The extraction of data on which experimentation is to be carried out is the courtesy of Fracture Technology Associates Laboratory which is a profitable, autonomous laboratory providing specimen testing facilities for about 40 years

- Different useful mechanical, physical and electrical properties for 2324-T39, 7055-T7511 and 6013-T651 Aluminum Alloys are mentioned in table 4.1, 4.2 and 4.3 respectively

- The fresh tentative data (ΔK, R and da/dN), which are attained from collected works, need to be carefully chosen and pre-processed prior to using it into the optimized neural network algorithms. This pre-processing includes natural logarithm of da/dN and ΔK followed by Normalizing $log\ da/dN$ and $log\ \Delta K$ attained previously

- A summary of the test conditions observed during experimentation process is shown in Table 4-4.

5. RESULTS AND DISCUSSION

This chapter presents the results of the research carrying the proposed technique. A thorough argument is presented on the performance of different machine learning algorithms used as a regression tool. Result of prediction of FCG rate has been presented in this. A comparison of the proposed technique with the experimental statistics is also presented.

5.1. Regression in Machine Learning

Regression has found imperative and large applications in machine learning and statistics. It permits to mark extrapolations from the existing data by having the knowledge of the connection concerning topographies of data and about experimental, continuous-valued reaction. Regression has got uses extending from forecasting stock rates to accepting genetic factor governing links. An unpretentious prototypical aimed at forecasting from a sole, invariant piece of the data is suitably called “simple linear regression”. Further than simple linear regression there is “multiple regression” in which several topographies of the information are made to use in establishing extrapolations.

From Figure 4.2, 4.3 & 4.4 it can be realized that there exists a non-linear comportment concerning input and output while focusing on Paris region. With the aim of perfectly forecasting this non-linearity, the three MLA founded Optimized Neural Networks are casted-off. For it, a practicable procedure to foretell FCG rate is familiarized that usages three MLA’s amongst Optimized Neural Networks. With the intention of authentication of the applied usefulness of the algorithms, the tentative information meant for diverse materials explicitly recycled for commercially sold aircrafts is taken out and engaged in the system of data sets. The three MLA based Optimized Neural Network are paralleled with each other and with formerly used MLAs for FCG rate prediction. For it, the 2-input and a 1-output prototypical is proven. This is completed by examining the corporeal

dynamic forces for FCG rate beneath constant amplitude loading. In this model SIF range"ΔK" and load ratio"R" are made in use as inputs and da/dN is engaged as output. The MLA based Optimized ANNs are authenticated on three diverse aluminum alloys, recycled for use in aircraft constructions. The tentative data of aluminum alloys for 4 dissimilar R-ratios is found and plotted using MATLAB. The plots are displayed in Fig. 4.2, 4.3 and 4.4. For precise extrapolation of non-linear presentation throughout FCG rate, the statistics are then randomized and separated keen on training and testing data sets wherever 70 % of data sections are casted-off for training and 30% are casted-off for testing and authentication of efficacy of Machine Learning Algorithms based Optimized Neural Networks.

The forecasted outcome in conjunction with the tentative outcomes is plotted for Optimized Neural Networks. Number of output statistics is kept on x-axis while output on y-axis for the above mentioned three aluminum alloys using diverse MLA techniques. Concerning Genetic Algorithm based Optimized Neural Network for 2324-T39 Aluminum Alloy; the plotted results are shown in Figure 5.1.

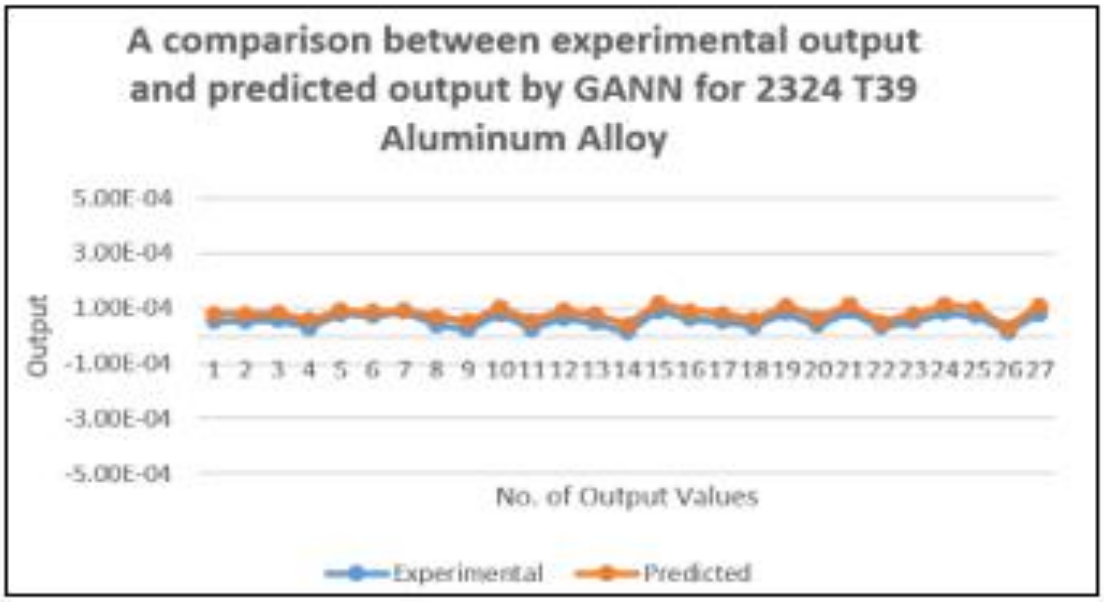

Figure 5.1. A Comparison of Experimental and Predicted Output Graph of Genetic Algorithm based Optimized Neural Network for 2324-T39 Aluminum Alloy

Similarly, the forecasted product in combination with the experimental outcomes is plotted for Hill Climbing based Optimized Neural Network. As in the previous case, number of output statistics is kept on x-axis while output on y-axis for afore presented three aluminum alloys using diverse MLA based techniques. With reference to Hill Climbing based Optimized Neural Network for 2324-T39 Aluminum Alloy; the plotted results are shown in Figure 5.2.

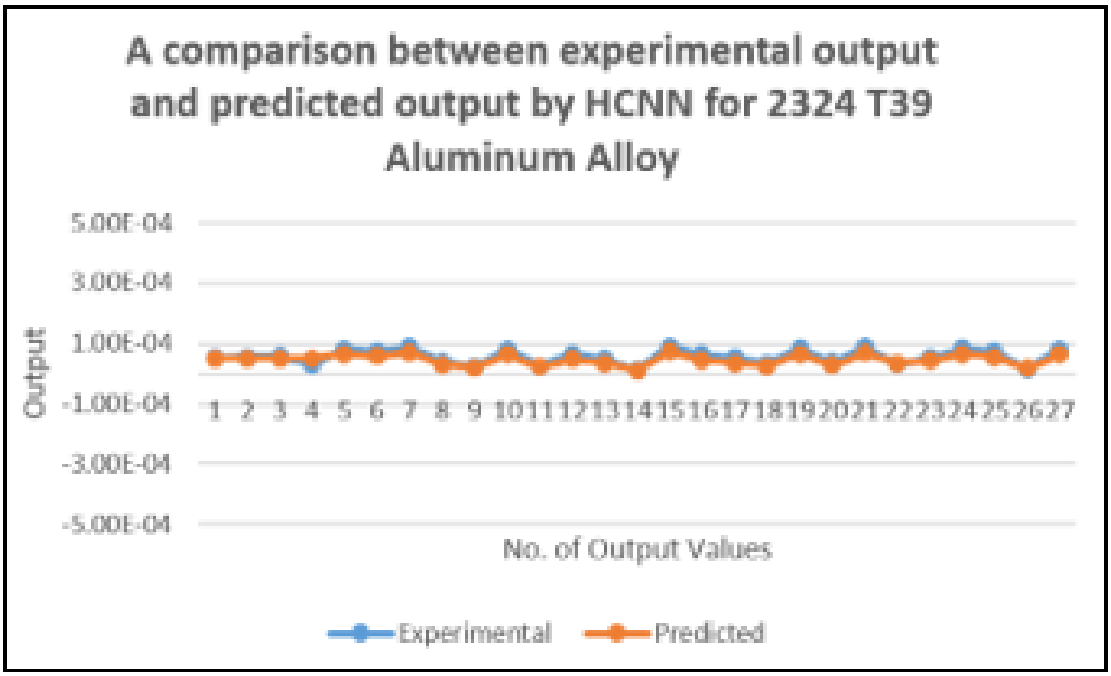

Figure 5.2. A Comparison of Experimental and Predicted Output Graph of Hill Climbing based Optimized Neural Network for 2324-T39 Aluminum Alloy

Likewise, the forecasted fallout together with the experimental results is plotted for Simulated Annealing based Optimized Neural Network. As in the preceding outcome, number of output information is kept back on x-axis whilst actual output on y-axis for three aluminum alloys mentioned earlier using three MLA based techniques. In connection with Simulated Annealing based Optimized Neural Network for 2324-T39 Aluminum Alloy; the plotted results are shown in Figure 5.3.

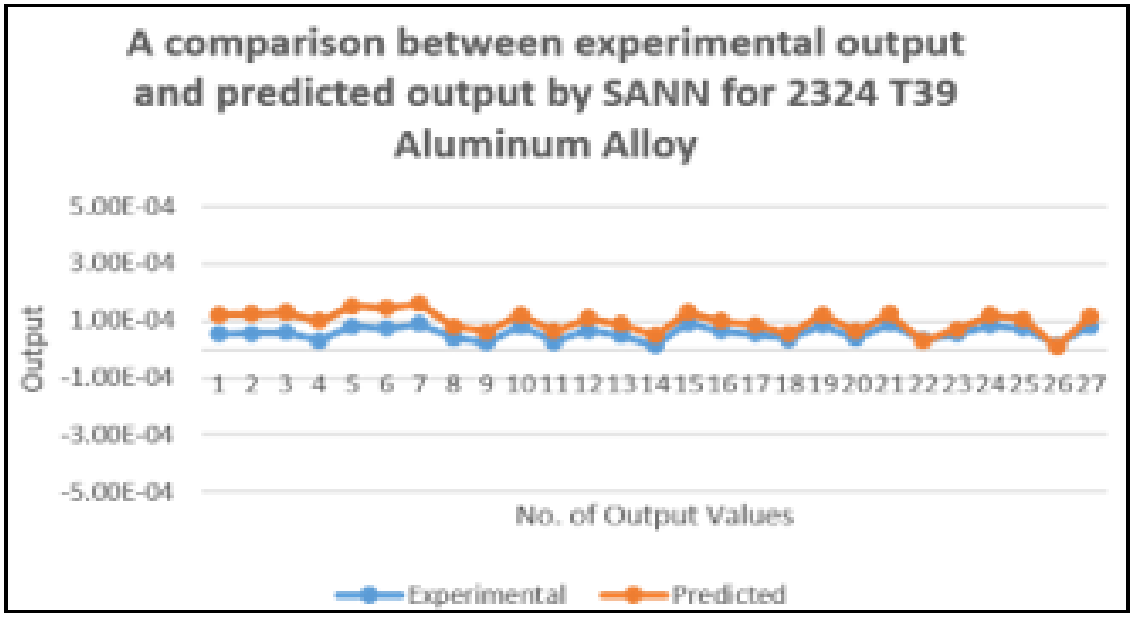

Figure 5.3. A Comparison of Experimental and Predicted Output Graph of Simulated Annealing based Optimized Neural Network for 2324-T39 Aluminum Alloy

It can be seen from Figure 5.1, 5.2 and 5.3 that there is a decent agreement involving experimental and forecasted output. Furthermore, it is experimented that at some points, the forecasted output curve overestimates the experimental amount produced curve. This is due to over-fitting of MLA based Optimized Neural Network. Over-fitting occurs where the prognostic representation depicts lofty discrepancy and stumpy partiality by reason of the noise in attendance of the data. It can be kept away from by corroboration and cross validation of the information and weighed against extrapolative accuracies continually.

Table 5.1 depicts abstract of the results of FCG Rate Prediction for 2324-T39 Aluminum Alloy using Optimized Neural Network Algorithms. Numbers of input layer neurons are two while there is a single output layer neuron accompanied with two hidden layer neurons. Training and predicted MSE's are also shown in Table 5.1 for 2324-T39 aluminum alloy when three algorithms are used that include GANN, HCNN and SANN.

Table 5-1: Results of FCG Rate Prediction for 2324-T39 Aluminum Alloy using Optimized Neural Network Algorithms

2324-T39 Aluminum Alloy					
Technique	**No. of Input Layer Neurons**	**No. of Hidden Layer Neurons**	**No. of Output Layer Neurons**	**Training MSE**	**Predicted MSE**
Genetic Algorithm Optimized Neural Network	2	2	1	7.1930×10^{-11}	3.6246×10^{-8}
Hill Climbing Optimized Neural Network	2	2	1	3.2043×10^{-11}	6.2171×10^{-9}
Simulated Annealing Optimized Neural Network	2	2	1	5.8576×10^{-10}	1.0559×10^{-9}

Among the three algorithms, Hill Climbing based Optimized Neural Network shows better results with MSE of $\mathbf{3.1069\times10^{-8}}$ followed by Genetic Algorithm based Optimized Neural Network and Simulated Annealing Optimized Neural Network respectively.
The structure of a feed forward network established is shown in Fig. 5.4.

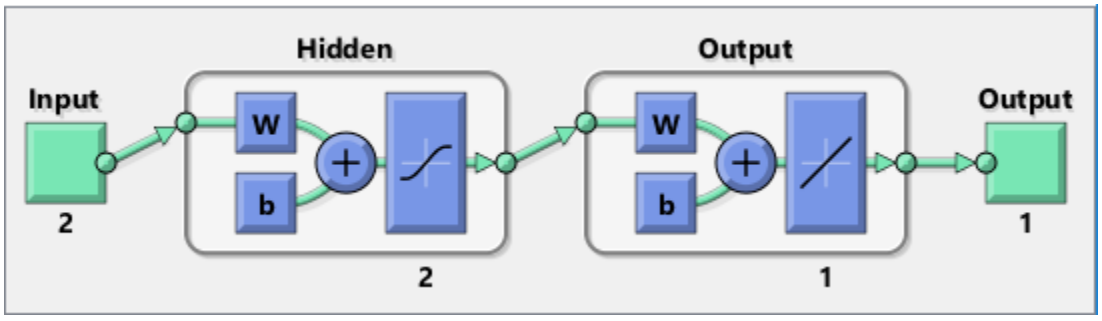

Figure 5.4. A structure of a Feed Forward Neural Network for 2324-T39 Aluminum Alloy

The forecasted output together with the tentative output is plotted for Genetic Algorithm based Optimized Neural Network. Number of output values is kept on x-axis while actual output on y-axis for the above mentioned three aluminum alloys using diverse MLA

techniques. Relating to Genetic Algorithm based Optimized Neural Network for 7055-T7511 Aluminum Alloy; the plotted results are shown in Figure 5.5.

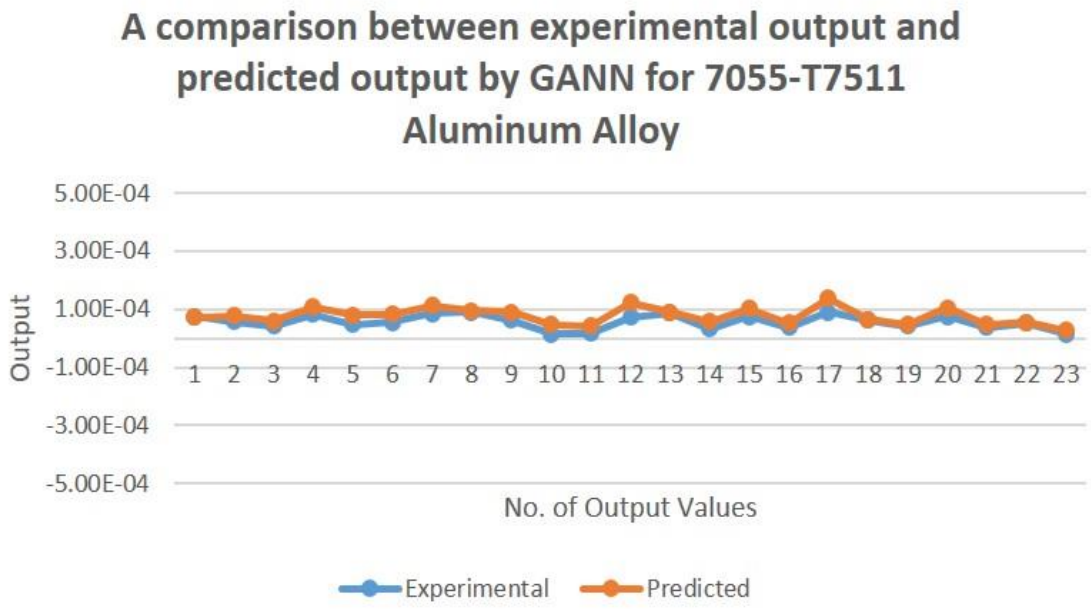

Figure 5.5. A Comparison of Experimental and Predicted Output Graph of Genetic Algorithm based Optimized Neural Network for 7055-T7511 Aluminum Alloy

Similarly, the forecasted product in association with the experimental outcomes is plotted for Hill Climbing based Optimized Neural Network. As in the previous case, number of output statistics is kept on x-axis while output on y-axis for afore mentioned aluminum alloys using various MLA based techniques. With reference to Hill Climbing based Optimized Neural Network for 7055-T7511 Aluminum Alloy; the plotted results are shown in Figure 5.6.

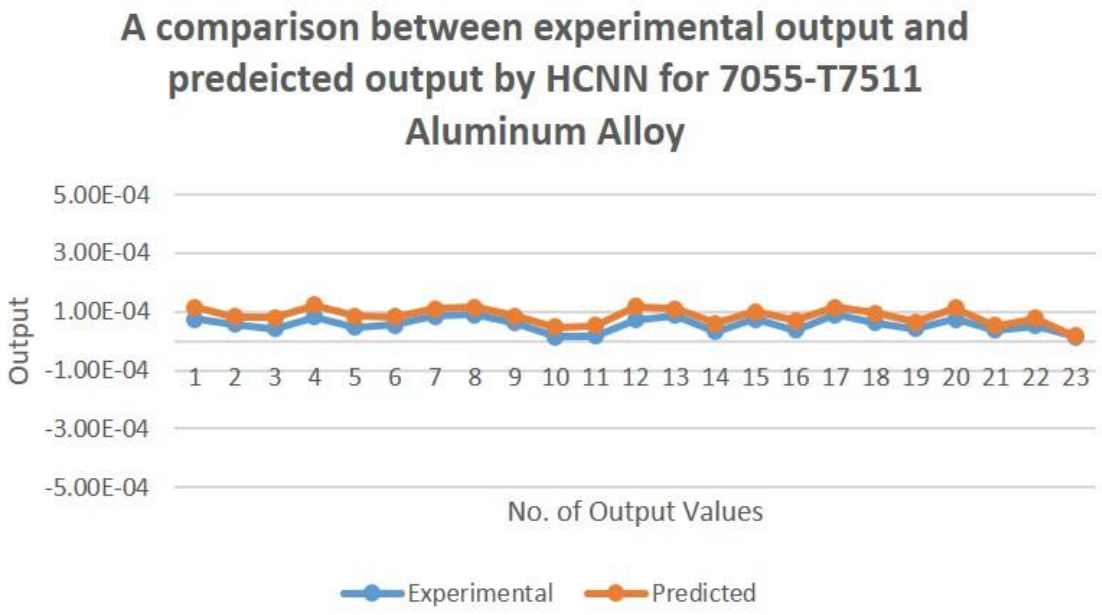

Figure 5.6. A Comparison of Experimental and Predicted Output Graph of Hill Climbing based Optimized Neural Network for 7055-T7511 Aluminum Alloy

Likewise, the predicted result against experimental output is plotted for Simulated Annealing based Optimized Neural Network. As in the preceding outcome, number of output information is kept back on x-axis whilst actual output on y-axis for three aluminum alloys mentioned earlier using three MLA based techniques. In connection with Simulated Annealing based Optimized Neural Network for 7055-T7511 Aluminum Alloy; the plotted results are shown in Figure 5.7.

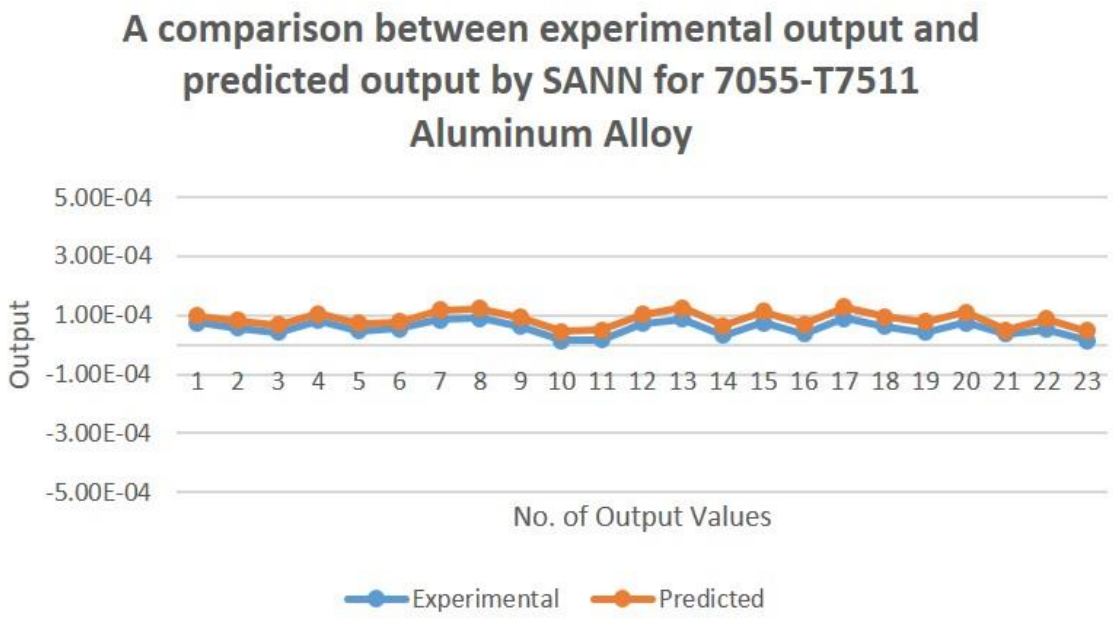

Figure 5.7. A Comparison of Experimental and Predicted Output Graph of Simulated Annealing based Optimized Neural Network for 7055-T7511 Aluminum Alloy

As observed in previous cases, it is clear from Figure 5.5, 5.6 and 5.7 that there is a decent concurrence linking tentative and predicted output. Furthermore, it is experimented that at some points, the forecasted output curve overestimates the experimental amount produced curve. This is due to over-fitting of MLA based Optimized Neural Network. Over-fitting occurs where the extrapolative demonstration depicts superior inconsistency and small partiality by reason of the noise in attendance of the data. It can be kept away from by corroboration and cross validation of the information and weighed against extrapolative accuracies continually.

Table 5.2 depicts abstract of the results of FCG Rate Prediction for 7055-T7511 Aluminum Alloy using various optimized neural network algorithms. Numbers of input layer neurons are two while there is a single output layer neuron accompanied with two hidden layer neurons. Training and predicted MSE's are also shown in Table 5.2 for 7055-T7511 aluminum alloy when three algorithms are used that include GANN, HCNN and SANN.

Table 5-2: Results of FCG Rate Prediction for 7055-T7511 Aluminum Alloy using Optimized Neural Network Algorithms

7055-T7511 Aluminum Alloy					
Technique	**No. of Input Layer Neurons**	**No. of Hidden Layer Neurons**	**No. of Output Layer Neurons**	**Training MSE**	**Predicted MSE**
Genetic Algorithm optimized Neural Network	2	2	1	1.3073×10^{-10}	6.6669×10^{-8}
Hill Climbing optimized Neural Network	2	2	1	8.3832×10^{-11}	1.4284×10^{-9}
Simulated Annealing optimized Neural Network	2	2	1	4.2147×10^{-10}	1.4512×10^{-8}

Among the three algorithms, Hill Climbing based Optimized Neural Network shows better results with MSE of $\mathbf{1.4284\times10^{-9}}$ followed by Simulated Annealing Optimized Neural Network and Genetic Algorithm based Optimized Neural Network respectively.
A view of a feed forward neural network for 7055-T7511 alloy is shown in Fig. 5.8.

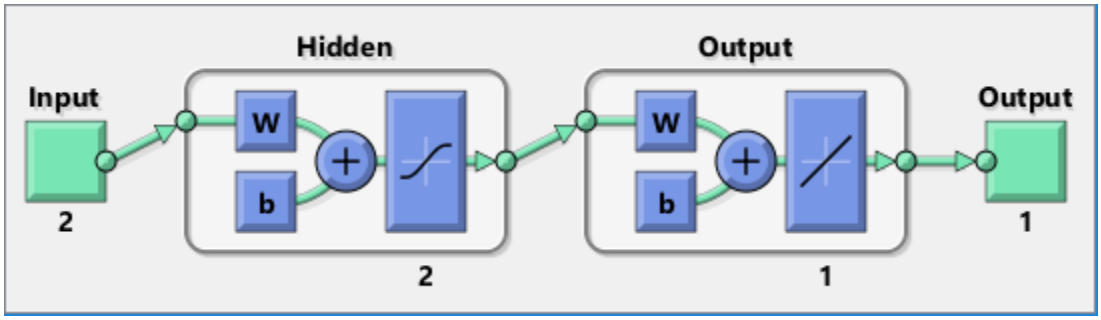

Figure 5.8. A structure of a Feed Forward Neural Network for 7055-T7511 Aluminum Alloy

The forecasted output together with the tentative output is plotted for Genetic Algorithm based Optimized Neural Network. Number of output values is kept on x-axis while actual

output on y-axis for the above mentioned three aluminum alloys using diverse MLA techniques. Relating to Genetic Algorithm based Optimized Neural Network for 6013-T651 Aluminum Alloy; the plotted results are shown in Fig. 5.7.

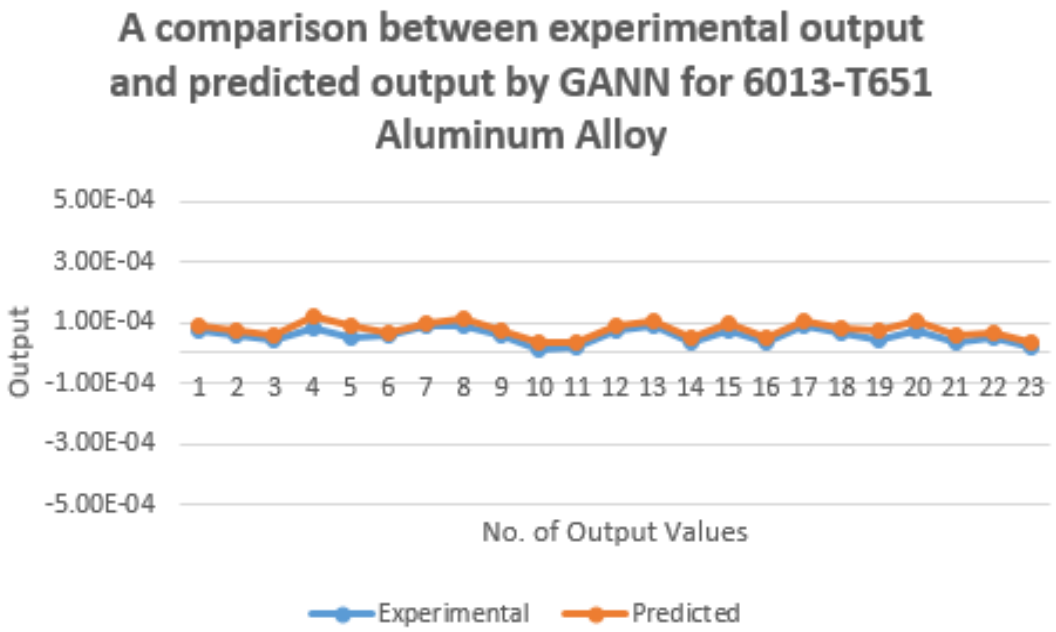

Figure 5.9. A Comparison of Experimental and Predicted Output Graph of Genetic Algorithm based Optimized Neural Network for 6013-T651 Aluminum Alloy

Similarly, the forecasted fallout in association with the experimental outcomes is plotted for Hill Climbing based Optimized Neural Network. As in the previous case, number of output statistics is kept on x-axis while output on y-axis for afore mentioned aluminum alloys using various MLA based techniques. With reference to Hill Climbing based Optimized Neural Network for 6013-T651 Aluminum Alloy; the plotted results are shown in Figure 5.10.

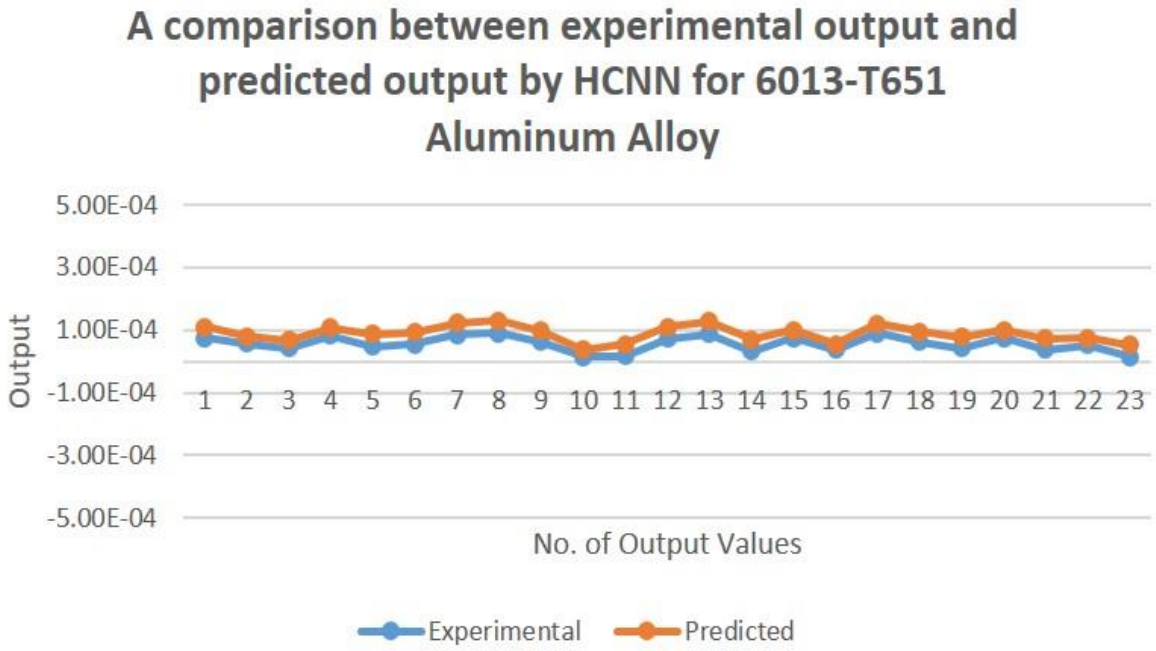

Figure 5.10. A Comparison of Experimental and Predicted Output Graph of Hill Climbing based Optimized Neural Network for 6013-T651 Aluminum Alloy

Likewise, the projected results against experimental output is plotted for Simulated Annealing based Optimized Neural Network. As in the preceding outcome, number of output information is kept back on x-axis whilst actual output on y-axis for three aluminum alloys mentioned earlier using three MLA based techniques. In connection with Simulated Annealing based Optimized Neural Network for 6013-T651 Aluminum Alloy; the plotted results are shown in Figure 5.11.

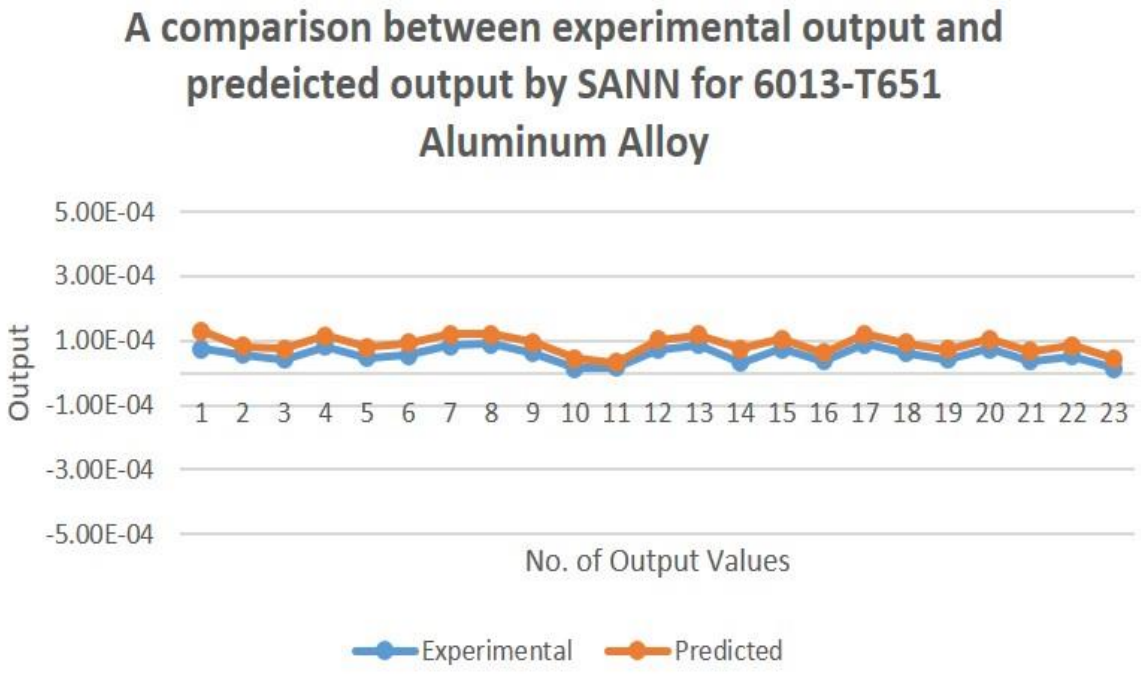

Figure 5.11. A Comparison of Experimental and Predicted Output Graph of Simulated Annealing based Optimized Neural Network for 6013-T651 Aluminum Alloy

As explained in the previous cases, it is clear from Figure 5.9, 5.10 and 5.11 that there is a decent concurrence linking tentative and predicted output. Furthermore, it is experimented that at some points, the forecasted output curve overestimates the experimental amount produced curve. This is due to over-fitting of MLA based Optimized Neural Network. Over-fitting occurs where the extrapolative demonstration depicts superior inconsistency and small partiality by reason of the noise in attendance of the data. It is possible to circumvent it by validating the output results over and over again and weighed against extrapolative accuracies continually.

Table 5.3 depicts abstract of the results of FCG Rate Prediction for 6013-T651 Aluminum Alloy using various optimized neural network algorithms. Numbers of input layer neurons are two while there is a single output layer neuron accompanied with two hidden layer neurons. Training and predicted MSE's are also shown in Table 5.3 for 6013-T651 aluminum alloy when three algorithms are used that include GANN, HCNN and SANN.

Table 5-3: Results of FCG Rate Prediction for 6013-T651 Aluminum Alloy using Optimized Neural Network Algorithms

6013-T651 Aluminum Alloy					
Technique	**No. of Input Layer Neurons**	**No. of Hidden Layer Neurons**	**No. of Output Layer Neurons**	**Training MSE**	**Predicted MSE**
Genetic Algorithm optimized Neural Network	2	2	1	6.4575×10^{-11}	1.1687×10^{-7}
Hill Climbing optimized Neural Network	2	2	1	5.5249×10^{-12}	3.1069×10^{-8}
Simulated Annealing optimized Neural Network	2	2	1	2.8805×10^{-10}	2.1515×10^{-7}

It can be inferred from Table 5.3 that amongst three algorithms, Simulated Annealing based Optimized Neural Network shows better results with MSE of $\mathbf{1.0559\times10^{-9}}$ followed by Hill Climbing based Optimized Neural Network and Genetic Algorithm based Optimized Neural Network respectively.

A view of a feed forward neural network for 7055-T7511 alloy is shown in Fig. 5.12.

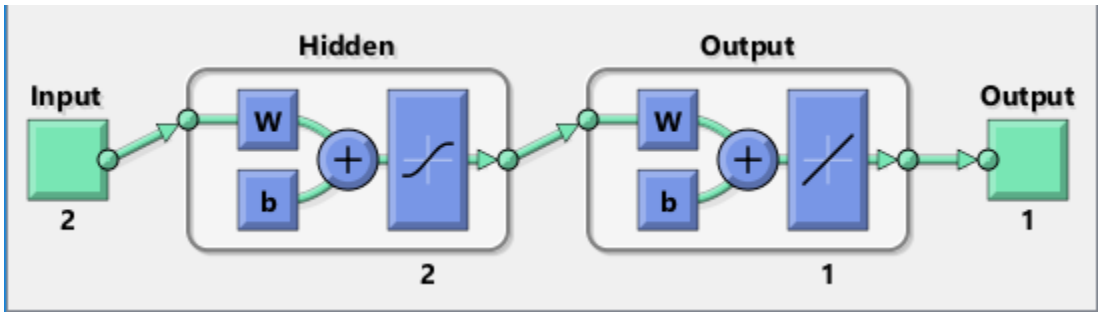

Figure 5.12. A structure of a Feed Forward Neural Network for 6013-T651 Aluminum Alloy

When all the algorithms in the proposed technique are taken into account, it can be inferred upon looking at the results that Simulated Annealing based Optimized Neural Network has given better results for 2324-T39 aluminum alloy when compared with others. The predicted MSE for SANN with 2324-T39 alloy is $\mathbf{1.0559 \times 10^{-9}}$.

5.2. Summary

The chapter can be summarized as follows:

- A thorough argument is presented on the performance of different machine learning algorithms used as a regression tool. A comparison of the proposed technique with the experimental statistics is also presented

- Regression has found imperative and large applications in machine learning and statistics. It permits to mark extrapolations from the existing data by having the knowledge of the connection concerning features of data and about experimental, continuous-valued reaction.

- The forecasted output together with the experimental output is plotted using Optimized Neural Networks. Number of output statistics is kept on x-axis while output on y-axis for 2324-T39, 7055-T7511 and 6013-T651 aluminum alloys using diverse MLA techniques

- For 2324-T39, Simulated Annealing based Optimized Neural Network shows better results with MSE of $\mathbf{1.0559 \times 10^{-9}}$ followed by Hill Climbing based Optimized Neural Network and Genetic Algorithm based Optimized Neural Network respectively. For 7055-T7511, Hill Climbing based Optimized Neural Network shows better results with MSE of $\mathbf{1.4284 \times 10^{-9}}$ followed by Simulated Annealing Optimized Neural Network and Genetic Algorithm based Optimized Neural Network respectively and for 6013-T651, Hill Climbing based Optimized Neural Network shows better results with MSE of $\mathbf{3.1069 \times 10^{-8}}$ followed by Genetic Algorithm based Optimized Neural Network and Simulated Annealing based Optimized Neural Network respectively

- When all the algorithms in the proposed technique are taken into account, it can be inferred upon looking at the results that Simulated Annealing based Optimized

Neural Network has given better results for 2324-T39 aluminum alloy when compared with others. The predicted MSE for SANN with 2324-T39 alloy is $\mathbf{1.0559 \times 10^{-9}}$.

- It is observed that at some points, the forecasted output curve overestimates the experimental outcome curve. This is due to over-fitting of MLA based Optimized Neural Network. Over-fitting occurs where the extrapolative demonstration depicts higher variation and small bias by reason of the noise in attendance of the data. It can be avoided from by validation and cross validation of the information and weighed against extrapolative accuracies continually.

6. CHALLENGES

Addressing the non-linearity accurately is the main concern of the research which is still found in infancy because of various limitations. The major challenge for undergoing experimentation is that the experimental setup is not readily available and demands hefty amount to avail the facility. Secondly, the specific material specimen to undergo experimentation is not easily obtainable.

As, benchmark data is used for experimentation and validation of results that was the courtesy of Fracture Technology Associates Laboratories. Over-fitting was seen in the results that is because of noise embedded in the data. It can be evaded by isolating the experimental setup from environment to achieve better results.

7. CONCLUSION AND FUTURE WORK

7.1. Conclusion

Material failure is an important and serious problem. Many accidents in the past are the result of failure of structures occurred due to excessive fatigue which has claimed lives of many people besides economic loss. Non-linearity in FCG curve is addressed using various analytical, hybrid and machine learning techniques in order to predict FCG rate perfectly. In an attempt to do so, in this research MLA based FCG prediction method is suggested. Optimized Neural Network based regression methodology is utilized in order to calculate and predict FCG rate with minimum error. Two input neurons and an output neuron is used to establish a network. SIF range and R-ratio for three alloys that are used in aircraft industry have been used as inputs of established optimized networks to predict FCG rate. A 2-input accompanied with 1-output network is trained against specific stopping conditions. Upon comparing results for three different commercially used alloys, it is observed that Hill Climbing based Optimized Neural Network shows better results when compared with other algorithms used in the proposed methodology for 2324-T39 aluminum alloy. For 7055-T7511 aluminum alloy as well, Hill Climbing based Optimized Neural Network has minimum predicted MSE as compared to Genetic Algorithm based Optimized Neural Network and Simulated Annealing based Optimized Neural Network. In contrast, Simulated Annealing based Optimized Neural Network shows better results for 6013-T651 aluminum alloy amongst other algorithms. Taking all the three algorithms used in the proposed technique into account for three alloys, it can be inferred upon looking at the results that Simulated Annealing based Optimized Neural Network has given better results for 6013-T651 aluminum alloy when compared with others. The predicted MSE for SANN with 6013-T651 alloy is$\mathbf{1.0559 \times 10^{-9}}$. The projected data displays a decent correspondence with experimental data and Optimized Neural

Networks address the non-linearities of FCG rate suitably. There is another observation upon viewing predicted and experimental curves that the extrapolative curves over-fits the experimental curves at various stages. This behavior of over-fitting can be evaded by cross confirmation of the data and calculating accuracies over and over again.

7.2. Future Work

Future work aims at optimizing data extraction used for training which include intensive experimentation on different materials upon availability combined with investigation of other MLA based optimized methods to achieve improved accuracy while forecasting FCG rate. Exploration of the appropriate methods and methodologies in order to overcome the challenges encountered in industrial use of the suggested technique are also included in future aims of the research.

7.3. Summary

The chapter can be summarized as follows:

- A novel MLA focused Optimized Neural Network based regression methodology is utilized in order to predict FCG rate with minimum error. A 2-input and 1-output network is trained against specific stopping conditions. Taking all the three algorithms used in the proposed technique into account for three alloys, it can be inferred upon looking at the results that Simulated Annealing based Optimized Neural Network has given better results for 6013-T651 aluminum alloy when compared with others. The projected data displays a decent correspondence with experimental data and Optimized Neural Networks address the non-linearities of FCG rate suitably.

- The behavior of over-fitting can be evaded by cross confirmation of the data and calculating accuracies over and over again.

- Future work aims at optimizing data extraction used for training combined with investigation of other MLA based optimized methods to achieve improved accuracy while forecasting FCG rate. Exploration of the appropriate methods and methodologies in order to overcome the challenges encountered in industrial use of the suggested technique are also included in future aims of the research

REFERENCES

[1] Dowling, N. E. (2012). Mechanical behavior of materials. *engineering methods for deformation, fracture, and fatigue. Pearson.*

[2] Beden, S. M. (2009). Review of fatigue crack propagation models for metallic components. . *European Journal of Scientific Research*, 28(3), 364-397.

[3] Paris, P. C. (1963, December). A critical analysis of crack propagation laws. . *ASME.*

[4] Forman, R. G. (1967). Numerical analysis of crack propagation in cyclic-loaded structures. . *Journal of basic Engineering*, 89(3), 459-463.

[5] Priddle, E. K. (1976). High cycle fatigue crack propagation under random and constant amplitude loadings. . *International Journal of Pressure Vessels and Piping*, 4(2), 89-117.

[6] Beden, S. M. (2009). Review of fatigue crack propagation models for metallic components. *European Journal of Scientific Research,*, 28(3), 364-397.

[7] Elber, W. (1971). The significance of fatigue crack closure. . *In Damage tolerance in aircraft structures. ASTM International.*

[8] Kujawski, D. (2001). A new (ΔK+ K max) 0.5 driving force parameter for crack growth in aluminum alloys. ,. *International Journal of Fatigue*, 23(8), 733-740.

[9] Donald, J. K. (1997). Introducing the K {sub max} sensitivity concept for correlating fatigue crack growth data. *The Minerals, Metals and Materials Society, Warrendale, PA (United States).*, (No. CONF-970980--).

[10] Sadananda, K. &. (1995). Analysis of fatigue crack closure and thresholds. *In Fracture Mechanics*, 25th Volume. ASTM International.

[11] Dinda, S. &. (2004). Correlation and prediction of fatigue crack growth for different R-ratios using K max and ΔK+ parameters. . *Engineering Fracture Mechanics,*, 71(12), 1779-1790.

[12] Sukumar, N. C. (2003). Extended finite element method and fast marching method for three-dimensional fatigue crack propagation. . *Engineering Fracture Mechanics*, 70(1), 29-48.

[13] Chopp, D. L. (2003). Fatigue crack propagation of multiple coplanar cracks with the coupled extended finite element/fast marching method. . *International journal of engineering science*, 41(8), 845-869.

[14] Bui, T. Q. (2014). Improved knowledge-based neural network (KBNN) model for predicting spring-back angles in metal sheet bending. International Journal of Modeling. *Simulation, and Scientific Computing*, 5(02), 1350026.

[15] Bhattacharya, S. S. (2013). Fatigue crack growth simulations of interfacial cracks in bi-layered FGMs using XFEM. . *Computational Mechanics*, 52(4), 799-814.

[16] Hu, X. B. (2017). A new cohesive crack tip symplectic analytical singular element involving plastic zone length for fatigue crack growth prediction under variable amplitude cyclic loading. . *European Journal of Mechanics-A/Solids*, 65, 79-90.

[17] Mohanty, J. R. (2015). Prediction of constant amplitude fatigue crack growth life of 2024 T3 Al alloy with R-ratio effect by GP. . *Applied Soft Computing*, 26, 428-434.

[18] Rodríguez, J. A. (2013). The use of artificial neural network (ANN) for modeling the useful life of the failure assessment in blades of steam turbines. *Engineering Failure Analysis,*, 35, 562-575.

[19] Rafiq, M. Y. (2001). Neural network design for engineering applications. . *Computers & Structures*, 79(17), 1541-1552.

[20] Venkatesh, V. &. (1999). A neural network approach to elevated temperature creep–fatigue life prediction. . *International Journal of Fatigue*, 21(3), 225-234.

[21] Artymiak, P. B. (1999). Determination of S–N curves with the application of artificial neural networks. . *Fatigue & Fracture of Engineering Materials & Structures*, 22(8), 723-728.

[22] Kang, J. Y. (1998). Neural network applications in determining the fatigue crack opening load. *International journal of fatigue,*, 20(1), 57-69.

[23] Haque, M. E. (2001). Prediction of corrosion–fatigue behavior of DP steel through artificial neural network. *International Journal of Fatigue* , 23(1), 1-4.

[24] Cheng, Y. H. (1999). Artificial neural network technology for the data processing of on-line corrosion fatigue crack growth monitoring. *International journal of pressure vessels and piping* ., 76(2), 113-116.

[25] Zio, E. &. (2012). Fatigue crack growth estimation by relevance vector machine. *Expert Systems with Applications* , 39(12), 10681-10692.

[26] Mohanty, J. R. (2015). Prediction of constant amplitude fatigue crack growth life of 2024 T3 Al alloy with R-ratio effect by GP. *Applied Soft Computing*, 26, 428-434.

[27] Zhang, W. B. (2016). An Artificial Neural Network-Based Algorithm for Evaluation of Fatigue Crack Propagation Considering Nonlinear Damage Accumulation. *Materials*, 9(6), 483.

[28] Wang, H. Z. (2017). A Comparison Study of Machine Learning Based Algorithms for Fatigue Crack Growth Calculation. *Materials*, 10(5), 543.

[29] Irwin, G. R. (1948). Fracture dynamics. *Fracturing of metals*, 152.

[30] Irwin, G. R. (1957). Analysis of stresses and strains near the end of a crack traversing a plate. *Journal of applied mechanics*, 24(3), 361-364.

[31] Fischer-Cripps, A. C. (2007). Linear Elastic Fracture Mechanics. *Introduction to Contact Mechanics*, 31-48.

[32] Orowan, E. (1997). Energy criteria of fracture.